SPIN WAVE DISPERSION RELATIONS IN THE DISORDERED FERROMAGNETIC FE-V ALLOYS

NOBORU SCHIBUYA

February 1978

CONTENTS

ABSTRACT

The spin wave dispersion relation in a body centered cubic disordered ferromagnetic alloy Fe-V has been measured by means of neutron inelastic scattering. The measurements were performed with the triple axis neutron spectrometer for the samples of Fe alloys containing 7.6, 8.7, 13.5, 16.0 and 18.7 atomic percent V over a wide range of the excitation energy from 5 to 60 meV at 290 K. Measured spin wave spectra are analysed with the equation of $E = D q^2(1 - \beta q^2)$ in the region of the large wave vector q and the stiffness constant D was determined for every specimen as well as the value of β. The observed values of D once increase with V concentrations from D = 290 meV $\AA^2$ for pure Fe, and tend to the value of about 400 meV $\AA^2$ for the alloy with high V concentration. In the low energy region, the spin wave spectrum deviates from the above equation. The magnitude of the deviation is larger for the specimens with smaller V concentration. The energy at which the deviation appears shifts from low to high as the concentration of V increases. For some specimens with high V concentrations, the deviation shows a maximum.

This kind of the anomaly observed in the spin wave excitation may be attributed to the effect of the impurity mode to the continuous spectrum and is the first example observed in a ferromagnetic disordered alloy.

I INTRODUCTION

In recent years much interest has grown to investigate the magnetic excitations in ferromagnetic transition metals and their alloys. Measurements of the spin wave spectrum of ferromagnetic transition metals Fe, Co and Ni have been made by neutron inelastic scattering over a wide range of the energy[1]-[3] by several authors. Theoretical works have been made to explain the experimental results of the spin wave dispersion relation and the recent calculation by Cooke and Davis is a successful example explaining a whole spectrum of spin wave excitation of Ni and Fe.[4],[5]

On the other hand, a small number of works has been made in the disordered ferromagnetic alloys both experimentally and theoretically. Measurements of the spin wave have been made only in f.c.c. Fe-Ni alloys and f.c.c. Ni-Co alloys for the relatively wide range of the excitation energy of up to 30 meV.[6]-[8] The spin wave stiffness constant D of ferromagnetic Fe based alloy Fe-Ni, Fe-Co, Fe-Cr and Fe-V has been determined for small wave vector q with the small angle and the diffraction method of neutrons by Harwell group.[9],[10]

Interest to investigate the spin wave excitations in the disordered ferromagnetic alloy consists of two aspects. One is the electron-atom ratio dependence of the stiffness constant D. The spin wave stiffness constant D of alloy is described with the exchange interactions between constituent atoms, J_{AA}, J_{BB}, J_{AB} in the AB binary alloy, and their magnetic moments in the Heisenberg model.

From the variation of D with the concentration of the alloy composition the exchange interactions can be obtained from the experiment as was often done in the Ni-Fe alloys.[7],[9] In the itinerant electron model the stiffness constant D depends on the average magnetic moment and the exchange band splitting and in a detailed way on the electronic band structure. The variation of D with alloying reflects the change of those parameters, which are theoretically to calculate. Early estimations of the variation of D in the Fe based 3d transition metal alloys were made with the rigid band model (R.B.M.) by Lowde et al.[10] The coherent potential approximation (C.P.A.) approachs on the calculation of D in the ferromagnetic alloy are recently developed and calculations of D in the Ni-Fe, Fe-Co, Fe-Cr alloys were made by Edwards and Hill[11], and Riedinger and Nauchiel-Bloch.[12]

The other subject is the possibility of an appearence of the anomaly in the spin wave spectrum, the resonance mode, due to introducing impurities. The existence of the localized or the resonance modes in the phonon spectrum has been experimentally confirmed in the disordered alloy systems[13] and the theoretical explanation has been also given.[14] In the magnetic system there exist almost no experimental works to investigate the impurity mode in the disordered alloy, except of the observation of the resonance mode by the inelastic incoherent neutron experiment in the Fe-Mn alloy.[15] Although the existence of the impurity mode is predicted theoretically in a single impurity case[16]-[18] the mechanism of the magnetic excitation in the disordered system has not been revealed at all.

In this paper the measurements of the spin wave excitations in the disordered ferromagnetic Fe-V alloy system have been reported. In this experiment the spin wave excitations were measured over a wide range of the excitation energy up to 60 meV with the triple axis neutron inelastic coherent scattering method.

The choice of the Fe-V alloy system as a sample is supported with the following experimental and theoretical informations. The b.c.c. Fe-V alloy is a ferromagnet, the transition temperature of which rises from that of Fe T_c= 1041 K with increasing the concentration of Vanadium atom. The average magnetic moment and the magnetic moments of individual atoms were experimentally obtained with the neutron magnetic elastic and the magnetic diffuse scattering experiments by Collins et al.,[19] Child and Cable,[20] and Yamashita et al.[21] Their results show that the average magnetic moment decreases as increasing the V concentration and the magnetic moment of Fe, however, remains almost constant value of about $2.2\mu_B$. Vanadium has a relatively large magnetic moment about $1.0\mu_B$, the direction of which is antiparallel to that of Fe at the low concentration of V up to 20 at.%. Such experimental results are theoretically well understood with the recent C.P.A. calculation by Kajzar,[22] and Hamada and Miwa.[23]

There exists no experiment on the whole spin wave spectrum. The stiffness constant D has been obtained with the diffraction method by Lowde et al.[10] The stiffness constant D is known to increase from the value of Fe with the concentration of Vanadium.

In Fe-V alloy the average moment decreases as a concentration of V, while the stiffness constant increases. In the other Fe based b.c.c. transition metal alloys the concentration variations of the average moment and the stiffness constant exhibit same tendencies qualitatively.

In the disordered ferromagnetic alloy the impurity to host spin ratio s/S and the impurity-host to host-host exchange ratio J'/J are the parameters of the possible excitation level of the impurity mode. In the disordered Ni-Fe ferromagnetic alloy the observation of a resonance mode has not been reported up to date. If the resonance mode really exists in Ni-Fe alloy, this will appear about the energy of 200 meV, that was estimated using the following values; J'/J= 0.3~0.5, E_{max} = 1250 meV and s/S = 4. The experimental difficulty prevents from observing such a high energy excitation.

In the Fe-V alloy system the reasonable ratio J'/J cannot be estimated from the concentration variation of D and T_c. The spin wave band width of Fe is accounted much smaller than that of Ni. In Fe-V alloy the fact that the spin of V atom is antiparallel to that of Fe is different to the case of Ni-Fe alloy. Fe-V alloy system may be different from the other 3d-transition metal alloys. From above mentioned informations the Fe-V alloy system is expected to have a large effect of V impurity in the spin wave spectrum.

The results of our experiment are analysed in two points of view mentioned above. The value of the stiffness constant D becomes larger compared with that of Fe, D_{Fe} = 280 meV $\AA^2$ at 290K with

increasing V concentration. This fact agrees well with the results of previous work.[10] The concentration dependence of D is explained qualitatively with R.B.M. The obtained spin wave spectrum cannot be described with the simple $E_q = Dq^2(1-\beta q^2)$ law and exhibits anomalous feature which may be due to the random magnetic impurities introduced in the ferromagnetic host.

In Sec. II the method of neutron inelastic scattering is briefly described. The sample preparation and the experimental detail with its analysis are described in Sec. III. The experimental results are discussed in Sec. IV.

II NEUTRON INELASTIC SCATTERING

The inelastic scattering of neutrons resulting from the creation or annihilation of a single spin wave quantum is subject to the conservation conditions for energy and momentum,

$$E_q = \frac{\hbar^2}{2m} (K'^2 - K_o^2)$$
$$\vec{K}_o + \vec{Q} = \vec{K}'$$
$$\vec{Q} = 2\pi\vec{\tau} + \vec{q}$$

where $\vec{K}_o$ and $\vec{K}'$ are the incident and final neutron wave vectors. The vector $\vec{q}$ is the wavevector of the spin wave and E is its excitation energy. $2\pi\vec{\tau}$ is a reciprocal lattice vector and $\vec{Q}$ is the scattering vector. With the triple axis spectrometer it is possible to vary one of two variables q and E, while the other is kept constant. The constant E scan is mainly employed for spin waves with high energy. This is due to the very high spin wave group velocity relative to the energy- momentum correlation of neutron, which is oblique in E-$\vec{q}$ plane with the slope of 4.144 K_o meV Å^{-1}, where $\vec{K}_o$ is the incident neutron wavevector. In contrast to phonon scattering experiment, $2\pi\vec{\tau}$ is limited to the first or second lowest Bragg reflections in the spin wave scattering because the scattered intensity decreases strongly with increasing $\vec{Q}$, due to the magnetic form factor.

The instrumental resolution corrections which arise because of the finite, rather large, size of the neutron probe in E-$\vec{q}$ space

must be always considered in the measurement of inelastic scattering, when the line width and the intensity of neutron groups will be discussed. We did not have aimed in this experiment to obtain the spin wave life time or the intensity. The resolution function is discussed by Cooper and Nathans.[24] Resolution function is given in the form,

$$R(\omega_o+\Delta\omega, \vec{Q}_o+\Delta\vec{Q}) = R_o \exp\left\{-\frac{1}{2}\sum\sum M_{kl} X_k X_l\right\}$$

$$X_1 = \Delta Q_x \ , \ X_2 = \Delta Q_y \ , \ X_3 = \Delta Q_z \ , \ X_4 = \Delta\omega$$

R_o is the optimum value of the resolution function $R(\omega_o, \vec{Q}_o)$. R_o and M_{kl} are involved functions of K_o, ω_o, Q_o and η_M, η_A, d_M, d_A, $\alpha_{i=0,3}$, $\beta_{i=0,3}$, where K_o is the wave vector of incident neutron. ω_o, Q_o are frequency and scattering vector. η_M, η_A are the horizontal mosaic spread of monochromator and analyser. α_0, α_1, α_2, α_3 and β_0, β_1, β_2, β_3 are the characteristic horizontal and vertical angle of the colimators and d_M, d_A the spacings of the monochromator and analyser. The dependence of the resolution function on $\Delta\omega$, $\vec{\Delta Q}$ is Gaussian. The locus of points in ω–Q space for which the resolution function has a value of half maximum is given by an ellipsoid,

$$\sum_{kl}\sum M_{kl} X_k X_l = 1.386,$$

which is refered as the resolution ellipsoid.

The observed intensity for a given scattering cross section σ is

$$I(\omega_c, Q_c) = \int R(\omega_o+\Delta\omega, R_c+\Delta R)\, \sigma(\omega_c+\Delta\omega, R_o+\Delta R)\, \Delta\vec{Q}\, \Delta\omega$$

For our experimental condition the resolution matrix M were calculated, using the expression in their text. Instrumental conditions were listed in Table I and calculated resolution ellipsoids at several energies and scattering vectors for TUNS and HB2 spectrometers are shown in Fig. 3(a). The resolution ellipsoid crosses the dispersion surface with a long principal axis almost perpendicular to it.

III Experiments and Results

(i) Sample Preperation

Five Fe-V samples of Vanadium concentration 7.6, 8.7, 13.5, 16.0 and 18.7 at. % were prepared in this experiment. The concentration range of specimens in the experiment is limited in b.c.c. phase. In the phase diagram of Fe-V alloy system γ-loop extends to about 2.0 at. % V. From 2.0 to 23.0 at. % Fe-V crystallizes in α phase and from about 23.0 at. % V σ phase is mixed to α phase. Raw materials of both 99.5 % Fe and V were melted together and grown into single crystal in the Bridgman furnace. The volume of the sample is 0.2~1.0 cc. Specimens of 7.6, 8.7 and 13.5 at. % were annealed at about 1000°C for a day. On 16.0 and 18.7 at. % V any thermal treatment was not made in order to avoid the mixing of σ phase. The concentration of 7.6 and 13.5 at % V was checked by chemical analysis and of others not yet done.

(ii) Experiments

The experiments were performed with the TUNS triple axis crystal spectrometer at JRR-2 and with the HB1A and HB2 triple axis spectrometers at the high-flux reactor HFIR at ORNL. Specimens of 7.6, 8.7 and 13.5 at. % V were measured at HFIR and of 13.5, 16.0 and 18.7 at. % V were measured at JRR-2. A neutron beam of fixed energies E_0= 33.0 meV and 29.8 meV was incident on the sample and the distribution of scattered neutrons was measured at JRR-2. Energy of scattered neutrons was fixed at E = 20.7, 24.8 and 41.4 meV with varying incident energies of neutrons

at HB2. Energy of incident neutron was fixed at E = 14.7 meV at HB1A.

As the dispersion curve is very steep in the ferromagnetic metals and alloys the constant energy mode of operation was taken with both neutron energy loss condition, i.e. spin wave creation in the sample, and neutron energy gain condition. Except in the sample of 8.7 at. % V two modes of the scan give the same dispersion curves. In the experiment trials are made to measure on the better condition, say, to obtain large intensities. The neutron cross section of the spin wave is written

$$\left(\frac{d^2\sigma}{d\Omega dE}\right) \propto \frac{K'}{K_0}\left\{(\langle n\rangle+1)\,\delta(E_q-E)\,\delta(\vec{Q}-\vec{q}-2\pi\vec{\tau}) + \langle n\rangle\,\delta(E_q+E)\,\delta(\vec{Q}+\vec{q}-2\pi\vec{\tau})\right\},$$

where $\langle n\rangle$ is the Boltzmann factor. In this experiment the intensity of scattered neutron was larger in the neutron energy gain condition than in the neutron energy loss condition. The reason is considered as follows. Considering the energy of incident neutron is 30 meV and the spin wave quantum of 20 meV is excited. The energy of scattered neutron is 10 meV for the energy loss process and 50 meV for the energy gain process. The spin wave creation process has a factor $\langle n\rangle+1$ and annihilation process has $\langle n\rangle$ in the cross section. At 300 K (above factor)$*(K'/K_0)$ is almost same in both processes. The main contribution to the intensity is attributed to the energy divergence of the scattered neutron to an angle. We measure $(d^2\sigma/d\Omega d\theta)$ instead of $(d^2\sigma/d\Omega dE)$ in the experiment. Both terms are related as follows

$$\left(\frac{d^2\sigma}{d\Omega d\theta}\right) \propto \frac{1}{\lambda^2 \tan\theta}\left(\frac{d^2\sigma}{d\Omega dE}\right)$$

The uncertainty of energy lead to larger angular divergence of scattered beam for the creation process than for the annihilation process.

Angular divergence of scattered beam is limited by the analyser to counter collimater and thus a reduction of neutron intensity takes place. The reflectivity of analyser may be saturated. The reflectivity is given

$$R = \frac{\lambda^4 F^2}{2 \sin^2\theta} V \quad .$$

The estimation of above mentioned values is made for both condition. From the results of the estimation we can see also that the measurement in the energy gain condition is better than that in the energy loss condition. The estimation is given in Table II and both measurements were compared in figure 1.

The (002) plane of pyrolitic graphite with mosaic spread of 25′ was used as a monochromator and an analyser on TUNS and HB1A. The (101) plane of Be crystal was used on HB2. Samples were mounted with [001] or [1$\bar{1}$0] crystal axis vertical and the scattering vector $\vec{Q}$ is on the plane vertical to its axis. The measurements were taken around the (110) Bragg point along [00ξ] direction or [$\xi\xi$0] direction of momentum transfer $\vec{q}$. Scans were taken on the focusing condition of the dispersion curve and resolution ellipsoid. The focusing effect is less sensitive in the experiment of the ferromagnetic metals having the steep dispersion from the reason mentioned in Sec.II. At the low excitation energy a large peak of LA phonon excitation covers the spectrum of the spin wave excitation. In order to avoid such a disturbance, scans were performed such as along [$\xi\bar{\xi}$0] direction from (110) Bragg point in the plane vertical [001] axis, in which geometry LA phonon was scarcely observed because of $\vec{e}\cdot\vec{Q}$ term in the cross section, where $\vec{e}$ is the polarization vector.

Both measurements along the [00ξ] and [ξξ0] direction almost coincide and an anisotropy of the excitation energy along the symmetry direction was not observed.

(iii) Results

The typical spectra obtained with constant E scan in each specimen are shown in figure 2. Measured range of energy transfer covers from 5 to 60 meV. Peaks of the observed spectra are all well defined.

Experimental full widths at half maximum of peaks for the samples of 7.6 and 18.7 at. % V are illustrated in figure 3(b). The condition measured is following. 7.6 at. % V was measured using Be monochromator and analyser. Scattered neutron energy was fixed and scans were taken along the [$\xi\bar{\xi}0$] direction. The FWHMs of pure Fe are also given for comparison which were taken in the same geometry as in 7.6 at. % V and give almost the instrumental resolution. 18.7 at. % V was measured with the different condition as before, that the (002) plane of PG was used as monochromator and analyser and incident neutron energy was fixed. Scans were performed along the [ξ00] direction with the spin wave annihilation condition. The resolution functions of the instrument are calculated and shown in figure 3(a). In figure 3(b) the straight line in the 18.7 at. % V sample represents the calculated width where the life time of spin wave is assumed to be infinite. The straight line in 7.6 at. % V is drawn as a guide for observed widths of Fe. The line width of spectrum may be whole due to the instrumental resolution. We can see slight deviations of measured widths from that of the resolution function around 10 meV in 7.6 at. % V and 20 meV in 18.7 at. % V, at those energies

dispersion curves have anomalies as shown later. We don't argue further about the line width, because measurements were performed with the loose instrumental condition without considering to discuss about the line width of observed spectrum.

The dispersion curve of each sample was obtained by taking the central point of scattered neutron distribution in wave vector transfer for each constant E spectrum. Backgrounds were suitably subtracted from observed intensities. The ambiguity of taking the central point of spectrum due to subtracting backgrounds was estimated at most as 0.005 $\mathring{A}^{-1}$ at low energy region, where phonon spectrum stands near the magnon peak. Obtained dispersion curves were shown in figure 4. The ambigutiy of determining the dispersion curve occurs also by statistical fluctuations of observed intensity. Measured intensity N at each wave vector point is assumed to have statistical deviations of $\pm 2\sqrt{N}$. The probability of finding intensity in this region is 0.95. All combinations of the possible intensities N, $N+2\sqrt{N}$ and $N-2\sqrt{N}$ at a certain wave vector point for all measured points M, thus 3^M sets of spectra, are taken. The distribution of the central wave vector q for all 3^M sets was made with the computer simulation. The full width at half maximum of this distribution function is small, about 0.005 $\mathring{A}^{-1}$ at the low energy of about 20 meV and 0.02 $\mathring{A}^{-1}$ at the high energy of about 50 meV. In figure 5 obtained points for ever constant E scan were plotted with error bar in the specimen of 13.5 at.% V, in which deviations in wave vector q from the fitted curve, as mentioned later, were shown. Although the obtained points scatter relatively, scattering is comparable with error bar as seen in figure and smaller than

the deviation of dispersion relation.

In figure 4 (f) dispersion relations in the 7.6 at.% V sample for the different symmetry directions [0ξ0], [$\bar{\xi}$00] and [ξ$\bar{\xi}$0] are shown with closed circles, cross points and open circles respectively. Any significant difference among them has not been observed at least up to 60 meV in the Fe-V alloy, as was also the case in Fe metal. Although the systematic measurements were not made, the anisotropy of the spin wave has not been detected for the other specimens beyond the experimental error.

The solid lines in figure 4 are the fitted curves to the equation $E = D\,q^2(1 - \beta q^2)$ with the procedure mentioned later. The dashed curves represent $E=Dq^2$ curves drawn using the D values obtained by Lowde et al.[10] In figure 4 (a) the dispersion curve of Fe obtained also in this experiment is shown as a comparison.

IV ANALYSES AND DISCUSSIONS

(i) Analyses of the experimental results

The excitation energy of the spin wave in the ferromagnetic metals and alloys is conveniently written as the power law

$$E = Dq^2(1-\beta q^2) \quad ,$$

where D is the spin wave stiffness constant and β is a parameter, which represents a deviation at large q from the quadratic dispersion relation. In order to obtain the stiffness constant D and β, E/q^2 values were plotted against q^2 for each concentration. E/q^2 versus q^2 curves are shown in figure 6. In the samples of lower concentration 7.6, 8.7 and 13.5 at.% V, E/q^2 values rise very steep for small values of q^2 and are almost linear to q^2 for large values of q^2. The rapid increase of E/q^2 around small values of q^2 may indicate whether the excitation energy has a finite gap at $q = 0$ or it has a dependence of wave vector in the first order. In rather concentrated samples of 16.0 and 18.7 at.% V, E/q^2 is nearly linear in the entire range of q^2. In the sample of 18.7 at.% V, moreover, E/q^2 points tend to deviate slightly downward from the straight line around small values of q^2. Extrapolating the straight line, which is the fitted curve to E/q^2 values around large values of q^2, to $q = 0$ we have obtained the stiffness constant D and β from the E/q^2 value at $q = 0$ and the slope of the straight line respectively. Obtained values of D and β for all specimens are given in Table III and plotted with the concentration of V in figure 7. Closed circles in figure 7 show present and open

circles previous results by Lowde et al., which were corrected at 290 K. Using obtained values of D and β the dispersion curves were drawn with the solid lines in figure 4 . The stiffness constants obtained in this experiment are somewhat larger than, but almost agree with those of Lowde et al. The value of D in the Fe-V alloy increases compared with that of Fe with the concentration of Vanadium.

As was mentioned above anomaly was observed at the low energy region. We next see, whether the excitation energy has a gap at q = 0 or the first order term in q. The dispersion relations were fitted to the equation: $E = E_0 + Dq^2(1 - \beta q^2)$, where E_0 denotes the energy gap, with E_0, D, β as the parameters. Obtained values of E_0, D, β are given in Table IV and illustrated in figure 9. As expected the dispersion curves have finite positive gaps at q = 0 in the specimens of 7.6, 8.7 and 13.5 at.% V, and a negative gap in the sample of 18.7 at.% V. In the concentration region of the positive energy gap obtained D and β become lower than those obtained by E/q^2 versus q^2 plot, and vice versa in the region of the negative energy gap.

E/q values were plotted against q, from which the dependence of the excitation energy on the first order term in q can be obviously seen, in figure 8. The situation was the same as before. In the samples of 7.6, 8.7 and 13.5 at.% V relation of E/q to q was drawn with the straight line: $E/q = C + Dq$ for small q region. Extrapolating to q = 0, E/q has a finite value, which means that the excitation energy has a dependence of the first order term in q. In the other specimens E/q crosses at the ori-

gin, and no q dependence was given. Obtained values of C and D were given in Table IV and illustrated in figure 9. If the first order term in q are taken into account, the value of D, of course, becomes smaller than that obtained before, assuming no or finite energy gap in the excitation energy.

Summarizing the analyses made above, it seems that the dispersion relation cannot be described simply with the $E = Dq^2(1 - \beta q^2)$ equation. If there exist anisotropic exchange interactions between spins, the excitation energy has a energy gap at $q = 0$. Such possibilities of having anisotropy however are little in 3d metals and their alloys. The excitation energy of spin wave has a Zeeman term in the magnetic field, but it is not the case in this experiment. Theexcitation energy depends on the first order in q at small q region in the case of antiferromagnet, it is also not the case. Therefore, it is difficult to explain that the excitation energy of spin wave has a finite gap at $q = 0$ or the first order dependence in q in the ferromagnetic Fe-V alloy.

In figure 10 deviations of measured points from the observed dispersion curve of Fe are plotted against the excitation energy of Fe. If the excitation energy is dependent on q as $E=Dq^2(1-\beta q^2)$ for both Fe metal and Fe-V alloy, and β s are assumed to be constant, the energy difference $E - E_{Fe}$ is in propotion to E_{Fe} and its constant is given by $(D/D_{Fe} - 1)$. In the Fe-V alloy $(D/D_{Fe} - 1)$ is positive as already seen. In the simply diluted ferromagnetic alloy such as Fe-Al alloy* $(D/D_{Fe} - 1)$ becomes

---

* The spin wave excitation in the Fe-Al alloy was recently measured by Y. Nakai et al. at HFIR at ORNL.

negative. We can see in figure 10 the difference $E - E_{Fe}$ is not propotional to E_{Fe} for the samples of small V concentration. In order to see this anomalous effect in detail, deviations of the dispersion relations from the fitted curve were also plotted against the wave vector q in figure 11. The dispersion relations deviate upward at the small q region in the lower concentration specimens, and are on the fitted curve in the 16.0 at. % V and become lower than that in the 18.7 at.% V specimen.

We have already seen that the deviation maximum locates around small q or E region and shifts from lower to higher energy as increasing V concentration, when the dispersion relation was fitted to the $E=Dq^2(1-\beta q^2)$ equation at the large wave vector region. Using Lowde's D deviations of measured points from the $E=Dq^2(1-\beta q^2)$ equation were replotted against the energy in figure 12. Its reason is that the diffraction method or the small angle method, with which only q^2 dependence of the excitation energy is measured, is more conventional than triple axis method for measuring D in the small q region. In the 18.7 at.% V deviations become upward around the energy of 20 meV, differing from in figure 11.

We next see, if the above equation describes well the dispersion relation at small q region, how alter the parameters such as D and β. In figure 5 another straight line can be drawn at small q^2 region, which gives larger D and β than those before, for example D = 600 meV and β = 9.0 $\mathring{A}^2$ in the 7.6 at.% V alloy. In this case the dispersion curve deviates largely at the high energy region or it seems as if there were two kinds of spin wave excitation, one of which propagates domi-

nantly with long wavelength and the other with short wavelength.

The possibility that this anomaly is attributed to the effect of coupling with phonon is ignored by the following reasons. First, any evidence of such anomaly has not been observed in pure Fe[2] and in the Fe-Si alloy[2], from which it seems that this effect is not due to introducing the impurity to cause a phonon -magnon interaction. In the relation to this fact, this anomaly disappears in alloys with V concentration higher than 16.0 at.%. If the phonon-magnon interaction is induced by impurity, its effect should be large at high impurity concentration.

This anomaly in the dispersion relation has not been observed in the disordered ferromagnetic alloy in which the spin wave measurements have been made up to date, such as in the Fe-Ni alloy or the Ni-Co alloy systems. This is first observed in the Fe-V alloy in this experiment. In some disordered ferromagnetic alloys the spin wave excitation energy may not be described with the simple wave vector dependence such as $E = D q^2(1 - \beta q^2)$. The excitation mode due to the magnetic impurity might be taken into account to understand the whole excitation spectrum.

(ii) Theoretical estimation of the stiffness constant

The estimation of the variation of D with the composition of constituent atoms is usually made with the Heisenberg model. In the disordered binary ferromagnetic AB alloy, considering the exchange interactions between constituent atoms as J_{AA}, J_{BB} and J_{AB}, the spin wave stiffness constant D is described as

$$D = 1/3\, z R_n^2 J_{eff}^{(2)} \bar{S}$$

$$J_{eff}^{(2)} \bar{S}^2 = c_A^2 S_A^2 J_{AA}^{(2)} + 2 c_A c_B S_A S_B J_{AB}^{(2)} + c_B^2 S_B^2 J_{BB}^{(2)}$$

$$\bar{S} = c_A S_A + c_B S_B$$

$$J_{AA}^{(n)} = z^{-1} \sum J_{AA}(r) \left(r/R_n \right)^n \quad ,$$

where R_n is a separation of the nearest neighbour atoms and $J_{AA}^{(2)}$ is the second moment of the exchange interaction J_{AA}. S_A and c_A are the spin and concentration of A atom respectively. Using the experimental values of S_{Fe} and S_V and the exchange interaction $J_{Fe-Fe}^{(2)}$, which was obtained in the Fe-Ni alloy by Hartherly et al.[9] and assumed concentration independent, the exchange interaction between Fe and V atoms $J_{Fe-V}^{(2)}$ was estimated. Assuming $J_{Fe-Fe}^{(2)}$ and $J_{Fe-V}^{(2)}$ to be concentration independent, $J_{Fe-V}^{(2)}$ must be chosen relatively large in order to explain the experimental results that the stiffness constant increases with V concentration. Result of estimation is given in Table V. If $J_{Fe-V}^{(2)}$ is chosen as $J_{Fe-V}^{(2)} = -4.0\, J_{Fe-Fe}^{(2)}$, an agreement can be obtained and it is illustrated in figure 6. Child and Cable have estimated $\left| J_{Fe-V}^{(0)} / J_{Fe-Fe}^{(0)} \right| \sim 2.8$ from the concentration dependence of $T_c^{(20)}$. $J_{Fe-Fe}^{(2)}$ may change with the concentration of V, since $J_{Fe-Fe}^{(2)}$ takes the contribution into account, not only of the nearest neighbour exchange interactions

but of long range interactions, and interacions between Fe atoms may be dependent on the configuration around Fe atom. The concentration variation of $J^{(2)}_{Fe-Fe}$ was obtained for $|J^{(2)}_{Fe-V}/J^{(2)}_{Fe-Fe}| = 0$ and 1, and illustrated in figure 13.It may be true in real system that $J^{(2)}_{Fe-V}$ is relatively large and also $J^{(2)}_{Fe-Fe}$ changes with the concentration of V.

Early calculations of the long wavelength spin wave energy in alloys, using the itinerant electron picture, were based on the rigid band model with suitably adjusted electron density of state and the exchange splitting. Following Wakoh's formulation[25] the stiffness constant D is given as follows,

$$D = \frac{1}{3m\Delta}\left[\frac{\Delta}{2}\{M(E_+)+M(E_-)\} - \int_{E_-}^{E_+} M(\epsilon)\,d\epsilon\right]$$

$$M(E) = \frac{V}{8\pi^3}\sum_{\lambda}\int_{E_{\lambda k}=E}\frac{|\nabla E_\lambda|}{}\,dS \quad ,$$

where Δ is the exchange band splitting, and E_+ and E_- are Fermi energies of up and down spin electron bands. m represents the average atomic magnetic moment of the alloy in Bohr magneton unit and λ is the 3d band index. V is the volume of the crystal. M(E) is a mean square velocity function and analogous to the usual density of state function N(E). He has calculated D of b.c.c. Fe using the band structure calculated by his own and above formula. In the case of the alloy the rigid exchange splitting is determined by the density of states of the based metal and the average magnetic moment in the rigid band model. In our estimation experimental values of the average moment in the Fe-V alloy and the calculated density of state curve N(E), and M(E) curve, which were used in the calculation

of b.c.c.Fe by Wakoh, were also used. The estimated concentration variation of D was drawn with the dashed curve in figure 7 and with the solid curve in figure 14, in which the value of pure Fe was normalized as a unit. The D increases as the Vanadium atoms are introduced in the Fe host also in the calculation. At the concentration of 10 at. % V the increase of D is about 20 % in the estimation, but 35 % in the experiment. The experimental value of D of Fe is 310 meV $\AA^2$ at 0 K. Wakoh's calculation of D however results to 80 meV $\AA^2$. A large discrepancy lies initially in Fe between the experiment and the calculation. An absolute value of D differs therefore by a factor 4 between the experiment and the calculation also in the case of the alloy. But the qualitative agreements are obtained between the experimental and R.B.M. results.

The increase of D with the V concentration is explained in detail in R.B.M. Because the spin of V is antiparallel to that of Fe, decrease of the average electron numbers due to introducing of V atoms results the decrease of the electron numbers of the majority or up spin band. This leads a large change of E_+ compared to E_- and the exchange band splitting energy is reduced in a large amount. On the other hand the area enclosed by M(E) curve and the straight line between $M(E_+)$ and $M(E_-)$, which is proportional to D from above equation, does not change so much. As a result the D becomes large. This feature is illustrated in figure 15.

C.P.A. approaches for calculating the stiffness constant D have been developed by several authors. In Ni-Fe alloy the calculated value of D by Riedinger and Nauchiel-Bloch agrees well with the experimental results.

(iii) Some remarks on β

Describing the spin wave dispersion relation phenomenologically $E = D q^2(1 - \beta q^2)$ in Heisenberg ferromagnet, β is given

$$\beta = \frac{1}{20} \frac{\sum_r J(r) r^4}{\sum_r J(r) r^2} ,$$

and in the case of binary alloy

$$\beta = \frac{1}{20} R_n^2 \frac{J_{eff}^{(4)} \bar{S}}{J_{eff}^{(2)} \bar{S}} ,$$

where expressions were same as in the previous section. Considering the interaction J only between nearest neighbours, β is only of dependence on a lattice spacing; $\beta = R_n^2 / 20$. In the case of Fe β is estimated as $0.3 \mathring{A}^2$ and experimental results was obtained as $1 \mathring{A}^2$. In the Fe-V alloy β changes little or slightly increases from the value of Fe with the concentration of V. This fact indicates that the long range interactions and the higher order moments in the q expansion of excitation energy must be taken into account. Since the stiffness constant D changes with the concentration of V, the biquadratic contribution of q becomes larger in the dispersion relation of Fe-V alloy than of Fe. These tendencies were also observed in Fe-4.0 at.% Si alloy, in which D decreased but β increased from those of Fe.

As a conclusion

(i) Anomaly of q dependence of the excitation energy was observed in the dispersion relation in the Fe-V alloy. The dispersion relation cannot be described with the simple $E = D\,q^2(1 - \beta q^2)$ equation. Its deviation from the above equation has a concentration dependence.

(ii) Anisotropy of the spin wave dispersion along the symmetry directions has not been observed up to 60 meV.

(iii) The stiffness constant D, obtained by fitting the dispersion relation to the above equation at large q region, rises from that of Fe with the concentration of V and tends to about 400 meV A^2 at about 15 at. % of Vanadium. Heisenberg model and the rigid band model were used in order to explain the experimental results. In the Heisenberg model $J^{(2)}_{Fe-V}$ was determined relatively large, if $J^{(2)}_{Fe-Fe}$ was assumed to be concentration independent. In the rigid band model the estimated concentration variation of D agrees at least qualitatively with the experimental results.

(iv) β changes slightly from the value of Fe $\beta_{Fe} = 1.0\ A^2$ with the concentration of V.

(v) The anomaly of dispersion seems not to be attributed to the magnon-phonon coupling.

Acknowledgements

The author wishes to express his sincere thanks to Prof. N. Kunitomi and Prof. Y. Nakai for their continual guidances and encouragements, and the fruitful discussions during the course of this study.

REFERENCES

(1) H. A. Mook and R. M. Nicklow: Phys. Rev. B7 (1973) 336.

(2) G. Shirane, V. J. Minkiewicz and R. Nathans: J. appl. Phys. 39 (1968) 383.

(3) H. A. Mook, R. M. Nicklow, E. D. Thomson and M. K. Wilkinson: J. appl. Phys. 40 (1969) 1450.

(4) J. F. Cooke and H. L. Davis: AIP Conf. Proc. 10 (1973) 1218.

(5) J. F. Cooke, J. W. Lynn and H. L. Davis: Solid State Commun. 20 (1976) 799.

(6) F. Menzinger, G. Gaglioti, G. Shirane and R. Nathans: J. appl. Phys. 39 (1968) 455.

(7) K. Mikke, J. Jankowska, A. Modrzejewski and E. Frikkee: Physica 86-88 B (1977) 345.

(8) K. Mikke, J. Jankowska and A. Modrzejewski: J. Phys. F6 (1976) 631.

(9) M. Hartherly, K. Hirakawa, R. D. Lowde, J. F. Mallet, M. W. Stringfellow and B. H. Torrie: Proc. Phys. Soc. 84 (1964) 55.

(10) R. D. Lowde, M. Shimizu, M. W. Stringfellow and B. H. Torrie: Phys. Rev. Lett. 14 (1965) 698.

(11) D. M. Edwards and D. J. Hill: J. Phys. F6 (1976) 607.

(12) R. Riedinger and M. Nauciel-Bloch: J. Phys. F5 (1975) 732.

(13) N. Kunitomi, Y. Tsunoda and Y. Hirai: Solid State Commun. 13 (1973) 495.

(14) for example W. Marshall and S. W. Lovesey: THEORY OF THERMAL NEUTRON SCATTERING Oxford university press 1971 p.528

(15) N. Kroo and L. Pal: J. appl. Phys. 39 (1968) 453.

(16) T.Wolfram and J. Callaway: Phys. Rev. 130 (1963) 2267.

(17) Yu. Izumov: Advan. Phys. 14 (1965) 569

(18) H. Ishii, J. Kanamori and T. Nakamura: Progr. Theoret. Phys. 33 (1965) 795

(19) M.F. Collins and G. G. Low: Proc. Phys. Soc. 86 (1965) 535

(20) H. R. Child and J. W. Cable: Phys. Rev. B13 (1976) 227

(21) O. Yamashita, Y. Yamaguchi and H. Watanabe: to be published in J. Phys. Soc. Japan

(22) F. Kajzar: J. Phys. F7 (1977) 1623

(23) N. Hamada and H. Miwa: to be published in Prog. Theor. Phys. 59 (1978)

(24) M. J. Cooper and R. Nathans: Acta. Cryst. 23 (1967) 357

(25) S. Wakoh: J. Phys. Soc. Japan 30 (1971) 1068

(26) Yung-Li Wang and H. Callen: Phys. Rev. 160 (1967) 358

(27) A.B. Harris and P. L. Leath, B. G. Nickel and R.J. Eliott: J. Phys. C7 (1974) 1693

(28) A. Theumann and R.A. Tahir-Kheli: Phys. Rev. B12 (1975) 1796

(29) A. T. Aldred: Intern. J. Magnetism 2 (1972) 223

TABLE CAPTION

Table I Instrumental conditions of neutron spectrometers.
α_0, α_1, α_2, α_3 represent horizontal collimation angles in degree of inpile, monochromator to sample, sample to analyser and analyser to counter respectively. η_M and η_A are mosaic spreads of monochromator and analyser in degree. d_M and d_A are the lattice spacing of monochromator and analyser in Angstrom.

Table II Comparison of scattered intensities in neutron energy loss and gain conditions.

Table III Concentration variation of D and β, obtained by E/q^2 versus q^2 plot at large q region. Values of Fe were also given for comparison.

Table IV Obtained parameters E_0, D, β and C, D
The dispersion relation is described $E = E_0 + Dq^2(1-\beta q^2)$ with energy gap E_0 and $E = Cq + Dq^2$ including q term

Table V Estimated values of stiffness constant D and $J_{Fe-Fe}^{(2)}$ taking suitable parameters in Heisenberg model

	E′(meV)	λ(Å)	θ(°)	$\lambda^4/SIN^2\theta$	K′/K₀	<n> or <n>+1	$COT\theta/\lambda^2$	RATIO	EXP
neutron energy loss	10	2.86	25.3	183.6	0.6	1.85	0.26	1	1
neutron energy gain	50	1.28	11.0	40.2	1.3	0.85	3.14	2.6	4

Table II

	α_0	α_1	α_2	α_3	η_M	η_A	d_M	d_A	
TUNS	0.5	0.5	0.5	0.5	0.4	0.4	3.354	3.354	PG(002)
HB2	2.0	0.67	0.67	5.0	0.3	0.15	1.733	1.733	Be(101)

Table I

V concentration at.%	D (meV Å^2)	β (Å^2)
7.6	385 ± 15	1.3
8.7	435 ± 25	2.2
13.5	370 ± 20	1.5
16.0	410 ± 20	1.2
18.7	440 ± 20	1.1
Fe	285	1.0

Table III

V concentration at.%	E_0 (meV)	D (meV Å^2)	β (Å^2)	C (meV Å)	D (meV Å^2)
7.6	2.8 ± 0.5	335.0 ± 2.0	0.9 ± 0.01	28 ± 7	243 ± 30
8.7	2.1	409.0	2.2	38 ± 7	226 ± 50
13.5	2.4	318.0	0.9	32 ± 9	217 ± 40
16.0	-0.5	448.0	2.0	0 ± 5	393 ± 10
18.7	-1.5	488.0	1.8	10 ±10	400 ± 20

Table IV

$$D = 1/3\ zR_n^2\ J_{eff}\bar{S}$$

$$J_{eff}^{(2)}\bar{S}^2 = c_{Fe}^2\ S_{Fe}^2\ J_{Fe-Fe}^{(2)} + 2c_{Fe}c_V S_{Fe}S_V\ J_{Fe-V}^{(2)} + c_V^2\ S_V^2\ J_{V-V}^{(2)}$$

$$\bar{S} = c_{Fe}S_{Fe} + c_V S_V$$

$$J_{Fe-Fe}^{(2)} = 18.2 \text{ meV}$$

$$J_{V-V}^{(2)} = 0$$

$$1/3\ zR_n^2 = 16.8$$

conc. V at.%	S_{Fe}	S_V	$1/3\ zR_n^2\ J_{Fe-Fe}^{(2)}\ c_{Fe}^2\ S_{Fe}^2$	$1/3zR_n^2$ $2c_{Fe}c_V S_{Fe}S_V J_{Fe-V}^{(2)}$ $\left\lvert J_{Fe-V}^{(2)}/J_{Fe-Fe}^{(2)}\right\rvert = 4.0$	D_{cal} (meV Å^2)	$J_{Fe-Fe}^{(2)}$ (meV) $\left\lvert J_{Fe-V}^{(2)} / J_{Fe-Fe}^{(2)}\right\rvert = 0$
5.0	1.05	-0.5	312	63	375	21.6
10.0	1.04	-0.41	299	105	404	25.1
15.0	1.03	-0.33	284	126	410	26.3
20.0	1.02	-0.27	269	144	412	28.1

Table V

FIGURE CAPTION

Figure 1 The distributions in wave vector transfer of scattered neutrons in the neutron energy loss and gain conditions. The energy of incident neutron is 29.8 meV. Neutron intensities in the case of the creation and annihitation of spin wave quantum, the energy of which is 19 meV, are illustrated.

Figure 2 The distributions in wave vector transfer of scattered neutrons from (a) 8.7, (b) 7.6, (c) 13.5, (d) 16.0 and (e) 18.7 at. % V Fe-V alloys at 290 K in constant energy scans at various energies. Peaks are all well defined. E_0 denotes the energy of incident neutron and E, of scattered neutron. The direction of scan is written in the figure.

Figure 3 (a) Calculated resolution ellipsoids in E-q space. The resolution ellipsoid is calculated at various E and Q on the dispersion surface. TUNS denotes the spectrometer used at JRR-2. HB 2 at HFIR at ORNL.

(b) Experimental line width (FWHM) of the spin wave excitation in 7.6 and 18.7 at. % V. In 7.6 at. % V the line widths are drawn with closed circles and the experimental line widths of Fe in the same condition were also plotted with open circles. The straight line is drawn for a guide to eyes. In 18.7 at. % V the widths of the calcutated instrumental resolution ellipsoids are drawn with the straight line. Associated instrumental conditions were listed in Table I.

Figure 4 The spin wave dispersion relations of Fe-V alloys, for (a) 7.6, (b) 8.7, (c) 13.5, (d) 16.0 and (e) 18.7 at.% V. The solid lines are drawn in the manner as discussed in the text. The dashed lines near the origin represent the dispersion curves with D values by Lowde et al. In figure 4 (a) the dispersion relation of Fe obtained also in this experiment is shown. In figure 4 (f) the spin wave dispersion relations are also given for various symmetry directions in 7.6 at.% V sample. Open and closed circles and cross points represent the measured points along $[\xi\bar{\xi}0]$ $[0\xi0]$ and $[\bar{\xi}00]$ directions respectively.

Figure 5 Experimental error in wave vector for various constant E scans. Scattering of obtained points is comparable with error bar and smaller than the deviation of dispersion

Figure 6 E/q^2 versus q^2 plot for each concentration of V. The straight lines are the fitted lines with E/q^2 values at large q^2. From the value of E/q^2 at $q = 0$ and the slope of the straight line, D and β are determined. E/q^2 values of Fe are also plotted with open circles.

Figure 7 Vanadium concentration dependence of the stiffness constant D and β at 290 K. Present values of D and β are shown with full circles and open circles represent the values of D by Lowde et al. for comparison. The solid line is drawn with taking $J^{(2)}_{Fe-Fe} = 18.2$ meV and $J^{(2)}_{Fe-V} = -4.0\, J^{(2)}_{Fe-Fe}$ in Heisenberg model as discussed in text. The dashed line is the estimated concentration variation of D with the rigid band model.

Figure 8 E/q versus q plot for each concentration of V. Extrapolating the heavy straight line to q=0, C and D are determined from E/q value at q=0 and slope of this line. The light straight lines were drawn with C=0 and D values obtained from E/q^2 versus q^2 plot.

Figure 9 Comparison of parameters obtained with different analyses: 1) $E = Dq^2(1-\beta q^2)$, 2) with energy gap E_0, $E = E_0 + Dq^2(1-\beta q^2)$ and 3) with q term, $E = Cq + Dq^2$.

Figure 10 Energy difference of the excitation energy of Fe-V alloys from that of Fe plotted versus the excitation energy of Fe. Straight lines indicate $E-E_{Fe} = (D/D_{Fe}-1)\ E_{Fe}$ equations. Deviation from the straight line is clearly seen.

Figure 11 Energy difference of the excitation energy of Fe-V alloys from the fitted curve plotted versus wave vector q. The curve was fitted to measured points at high energy region as discussed in text.

Figure 12 Energy deviations of the excitation energy of Fe-V alloys from the calculated curves with using D's by Lowde et al.

Figure 13 Concentration variation of $J^{(2)}_{Fe-Fe}$. The cases of $|J^{(2)}_{Fe-V} / J^{(2)}_{Fe-Fe}| = 0$ and 1 are shown.

Figure 14 Reduced stiffness constant D/D_{Fe} versus V concentration. Estimated concentration variation of D/D_{Fe} using RBM is drawn wuth the solid line. The concentration variation of T_c is also shown with the dashed line.

Figure 15 Concentration variation of the band splitting energy and area enclosed M(E) curve and the straight line between $M(E_+)$ and $M(E_-)$ in the Fe-V alloy in RBM.

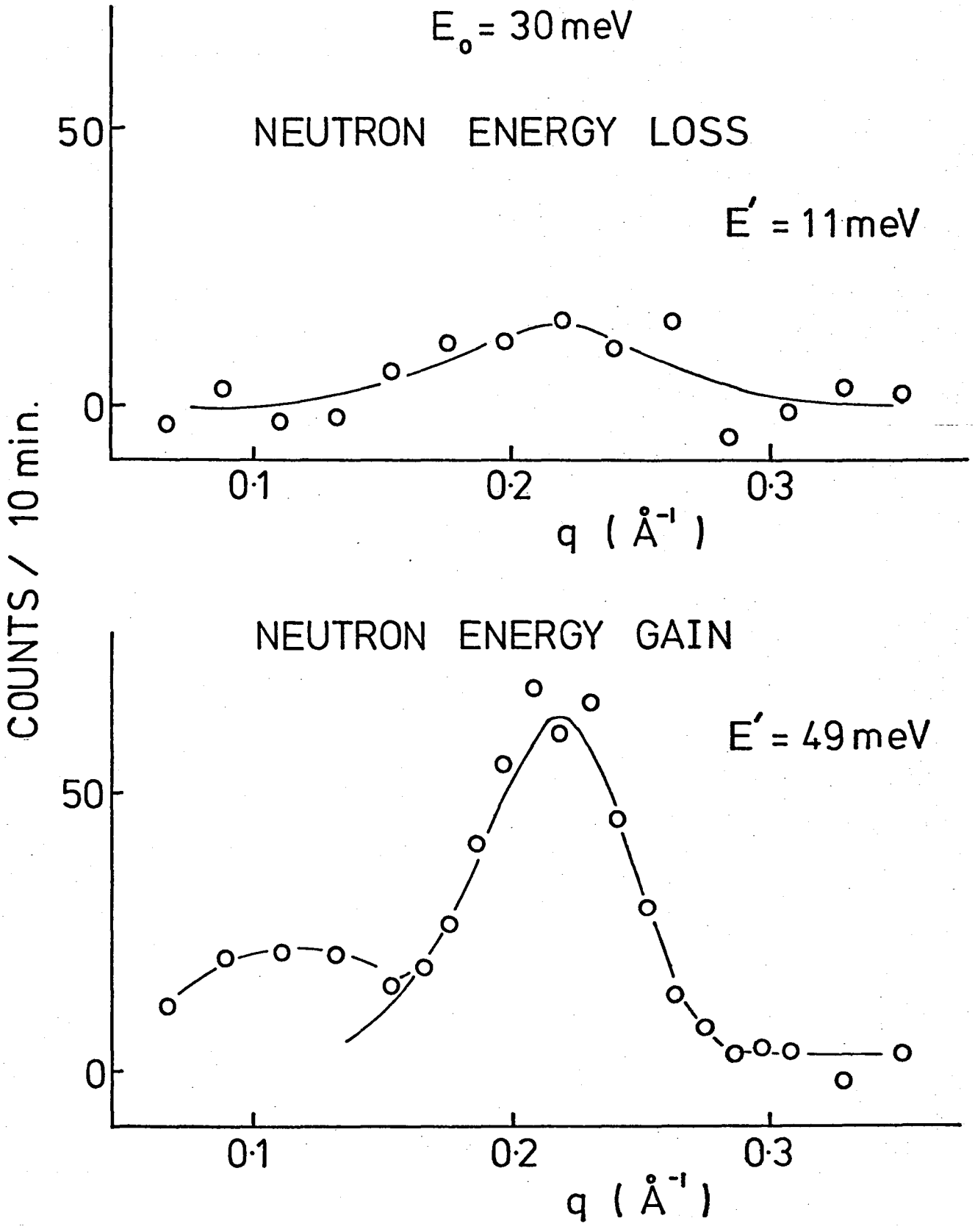
E_o = 30 meV
NEUTRON ENERGY LOSS
E′ = 11 meV
50
0
0·1
0·2
0·3
q (Å^{-1})
COUNTS / 10 min.
NEUTRON ENERGY GAIN
E′ = 49 meV
50
0
0·1
0·2
0·3
q (Å^{-1})

FIGURE 1

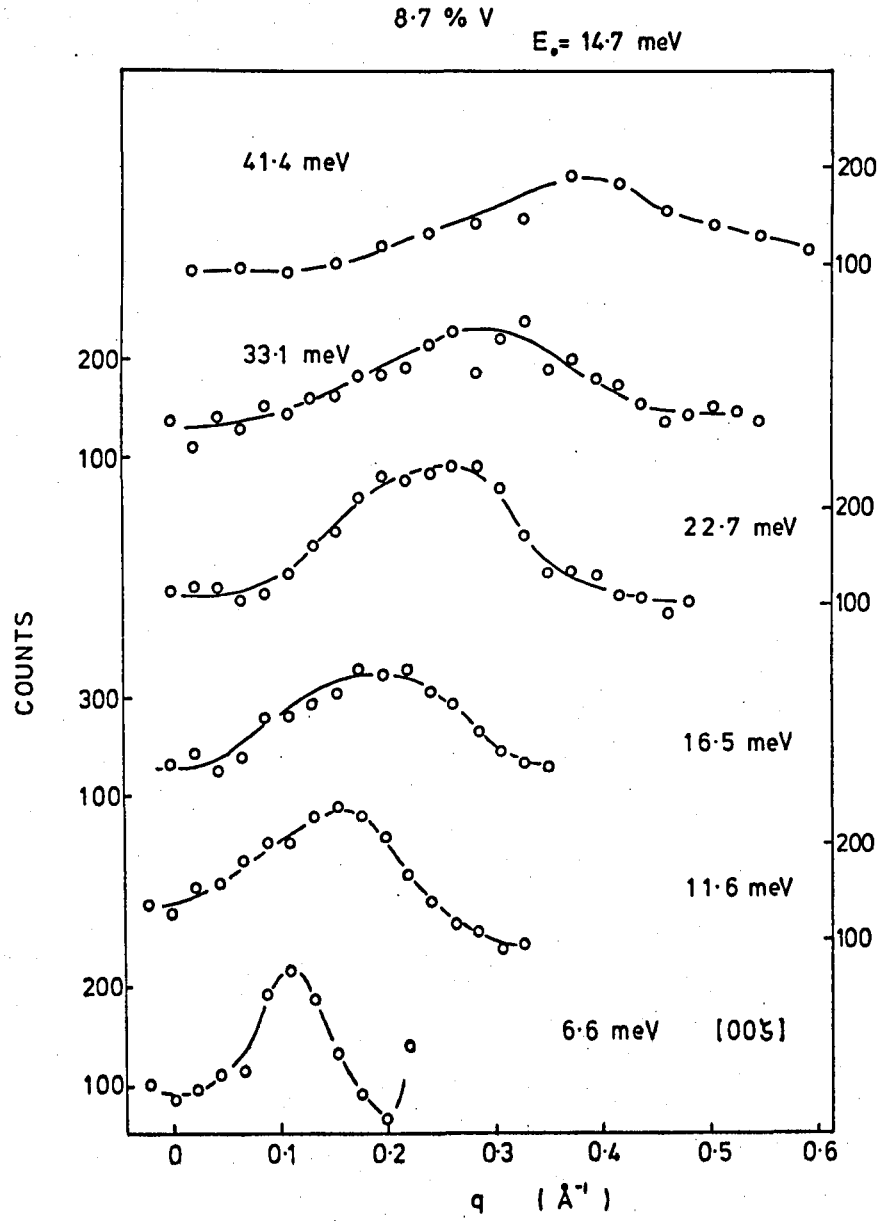

FIGURE 2 (a)

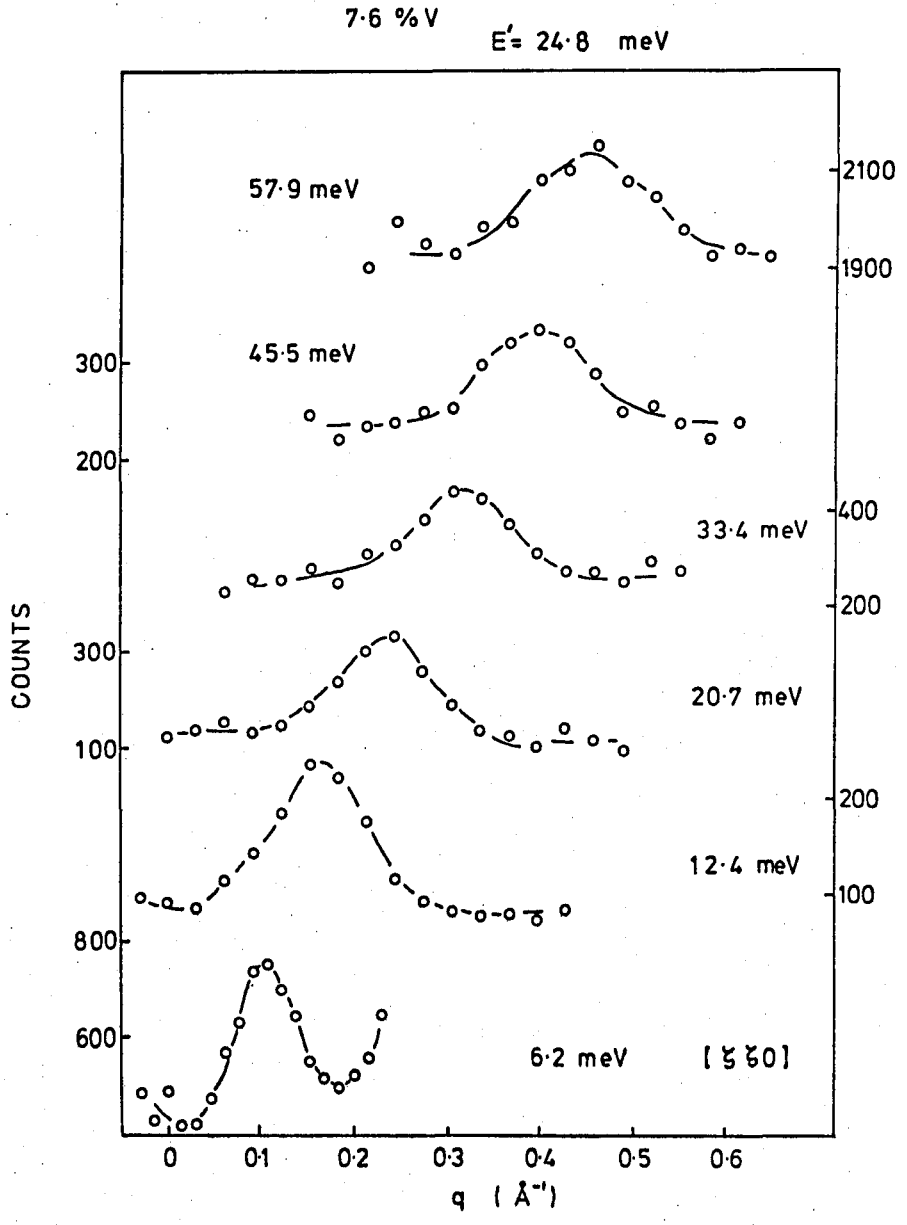

FIGURE 2 (b)

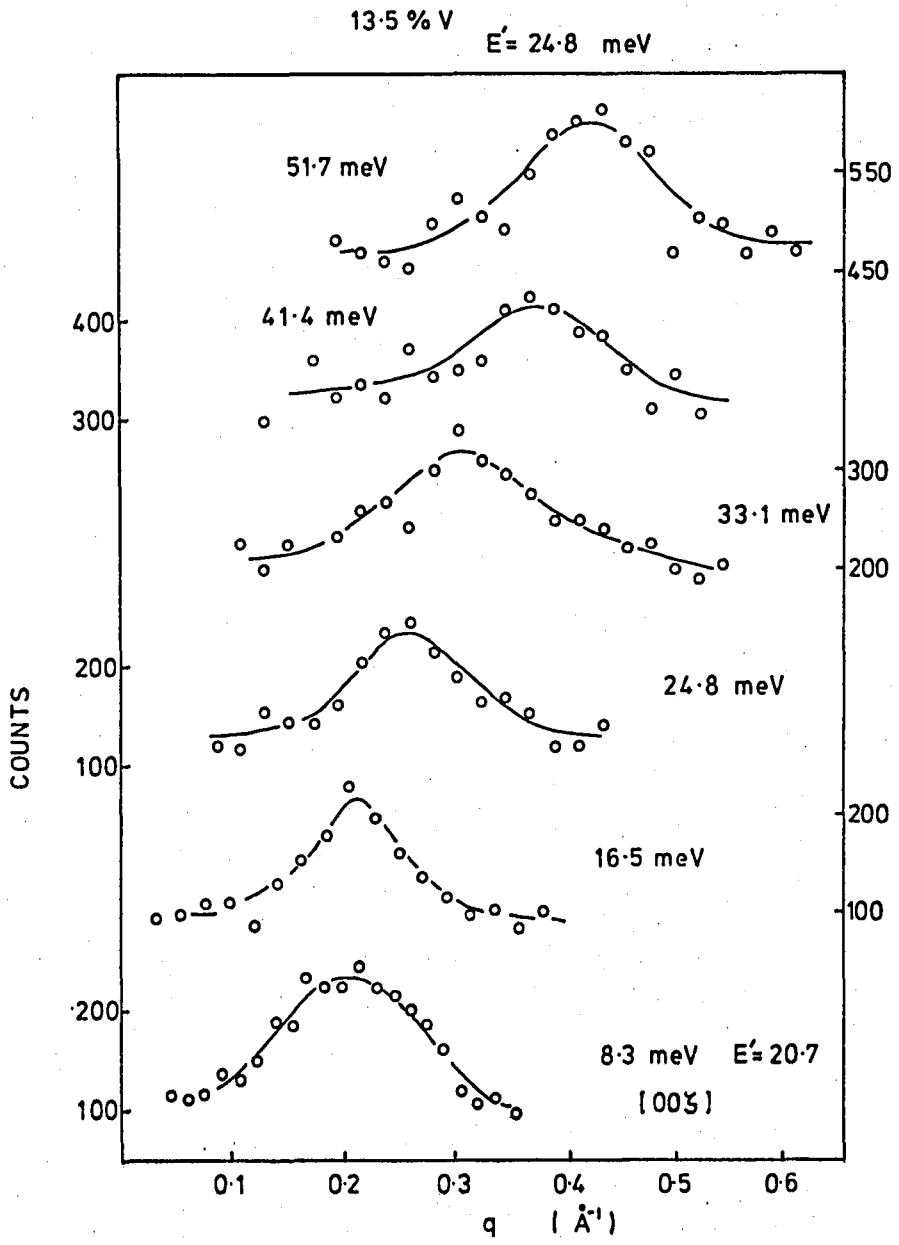

FIGURE 2 (c)

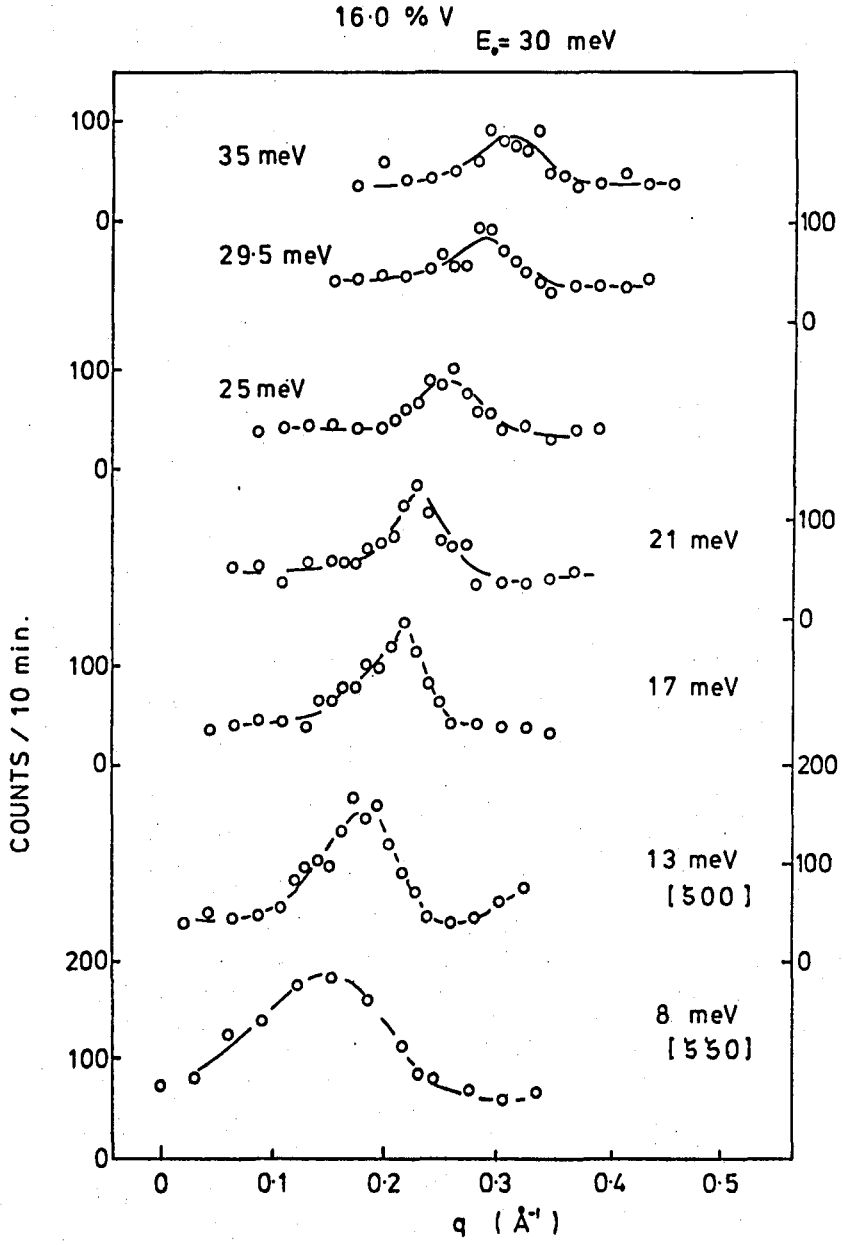

FIGURE 2 (d)

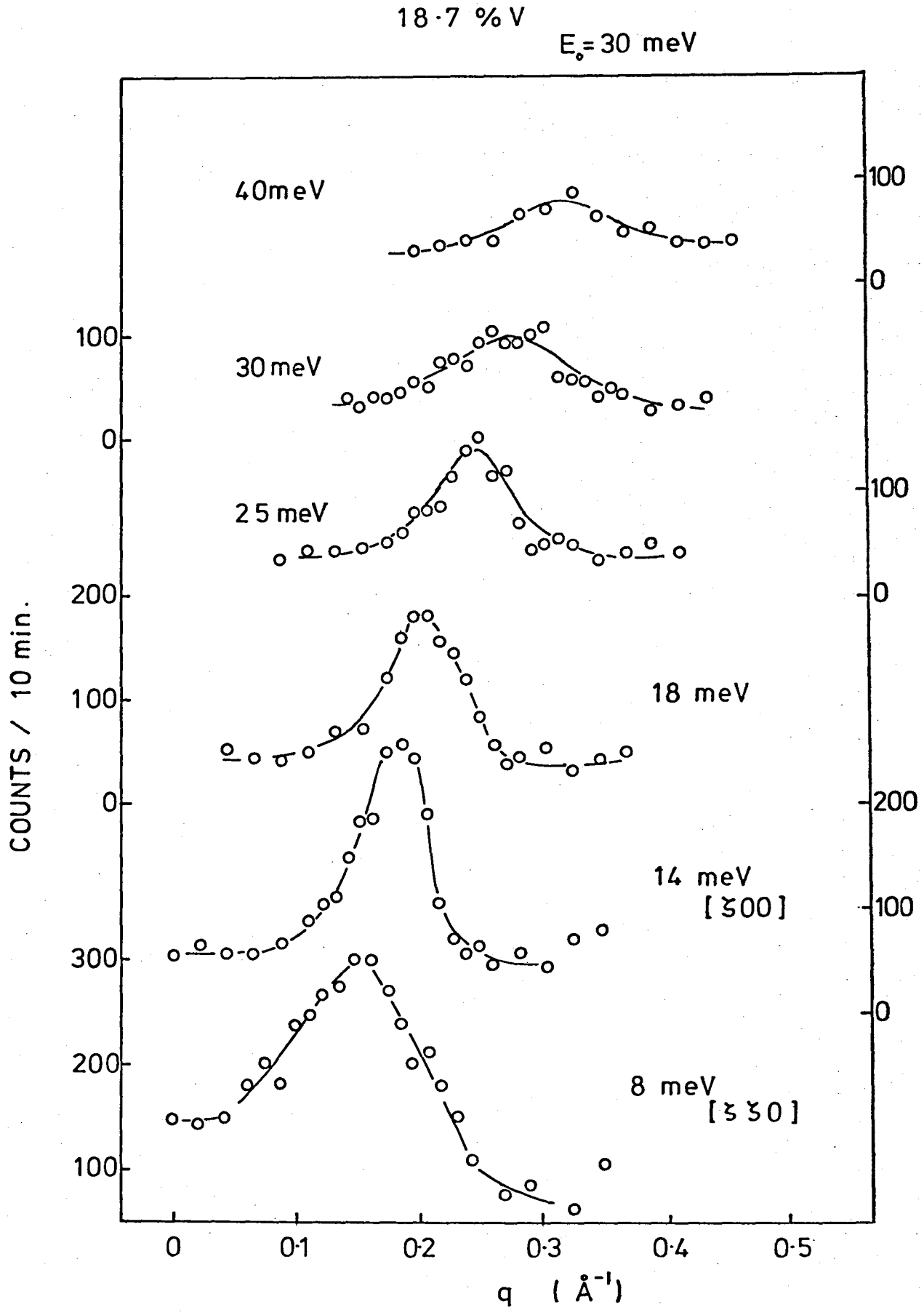
18·7 % V
E₀ = 30 meV
40meV
30 meV
25 meV
18 meV
14 meV
[ξ00]
8 meV
[ξξ0]
COUNTS / 10 min.
q (Å⁻¹)
0
0·1
0·2
0·3
0·4
0·5

FIGURE 2 (e)

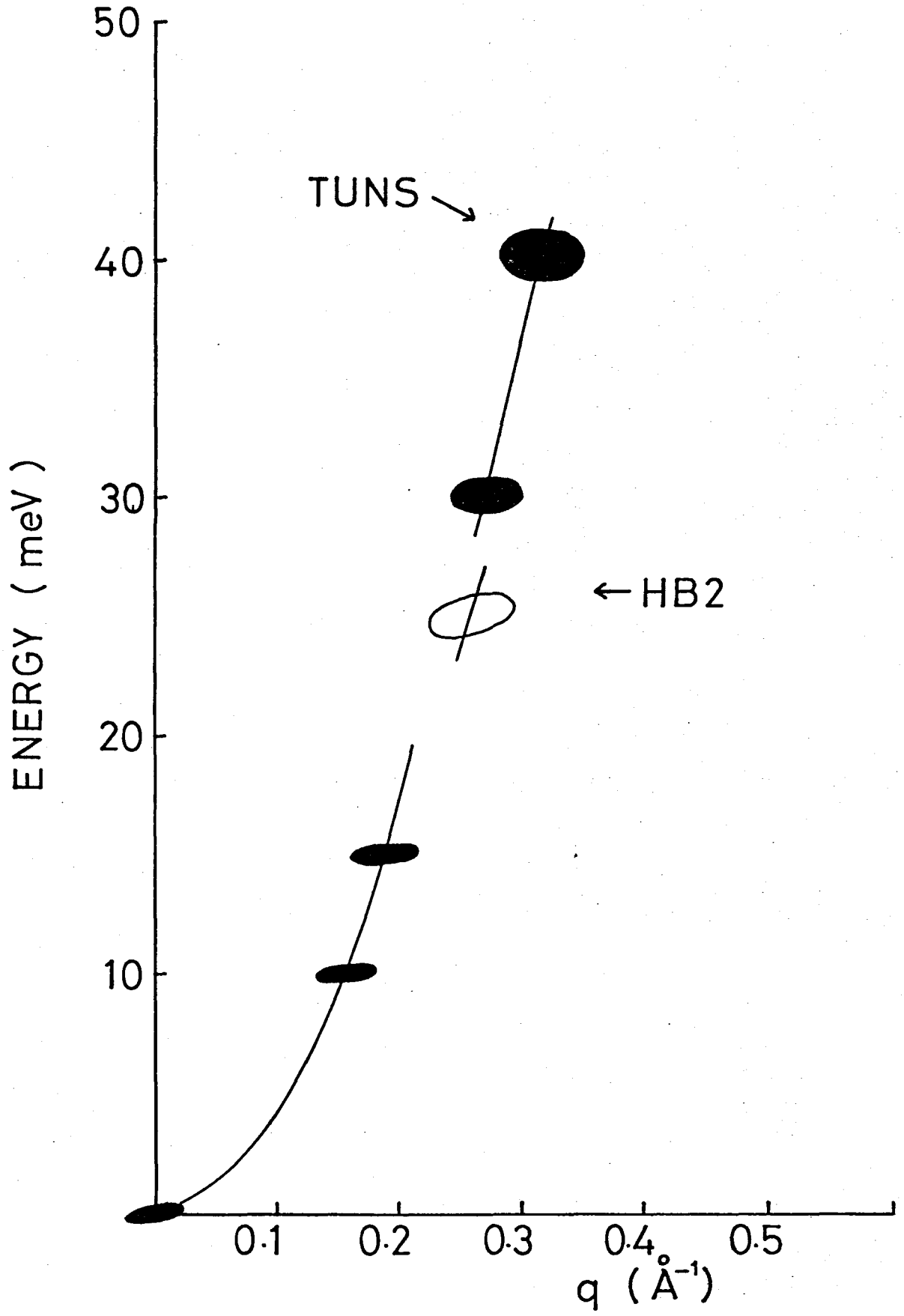

FIGURE 3 (a)

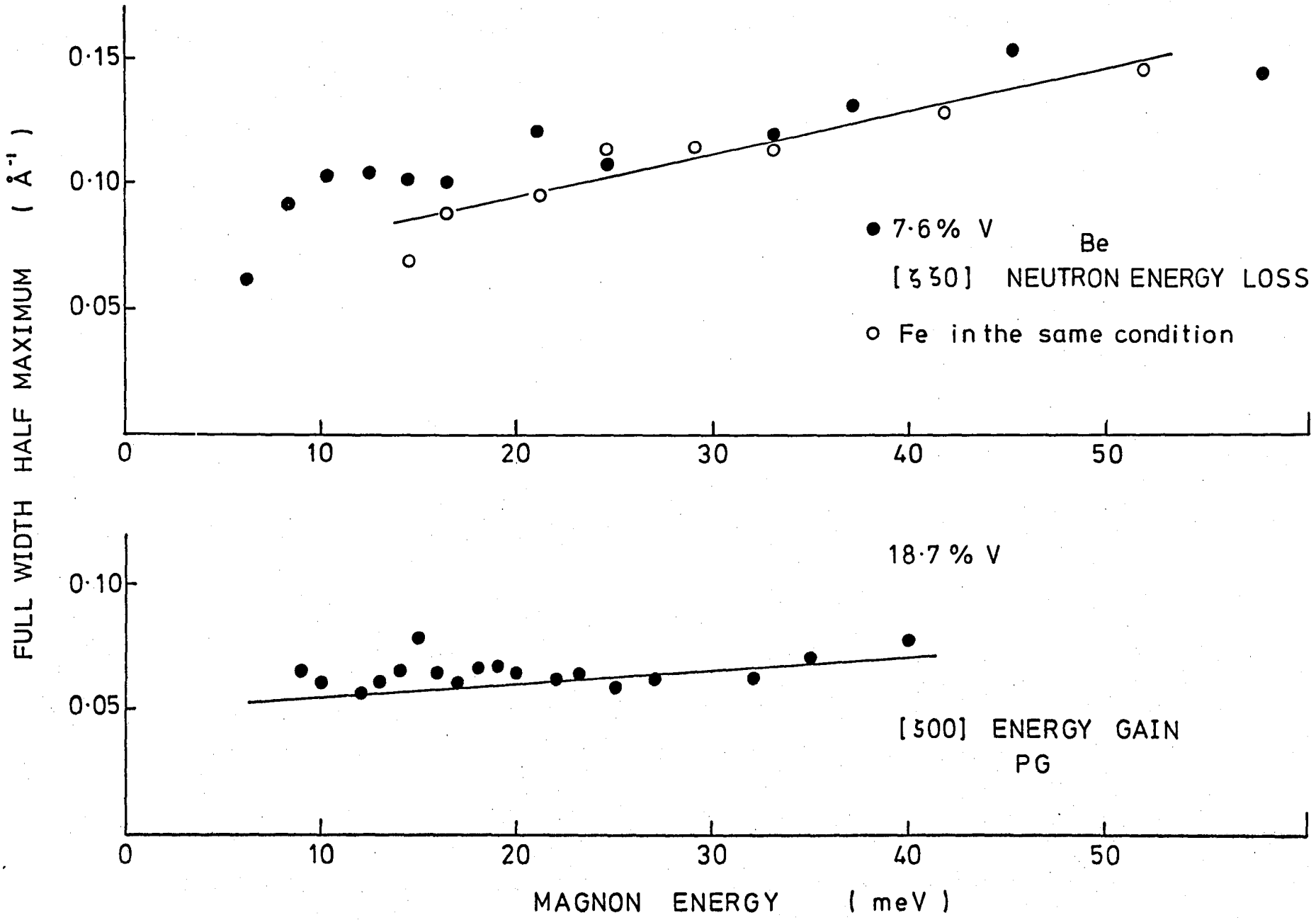
FULL WIDTH HALF MAXIMUM (Å⁻¹)
0·15
0·10
0·05
0
10
20
30
40
50
● 7·6 % V
Be
[330] NEUTRON ENERGY LOSS
o Fe in the same condition
18·7 % V
0·10
0·05
[500] ENERGY GAIN
PG
MAGNON ENERGY (meV)

FIGURE 3 (b)

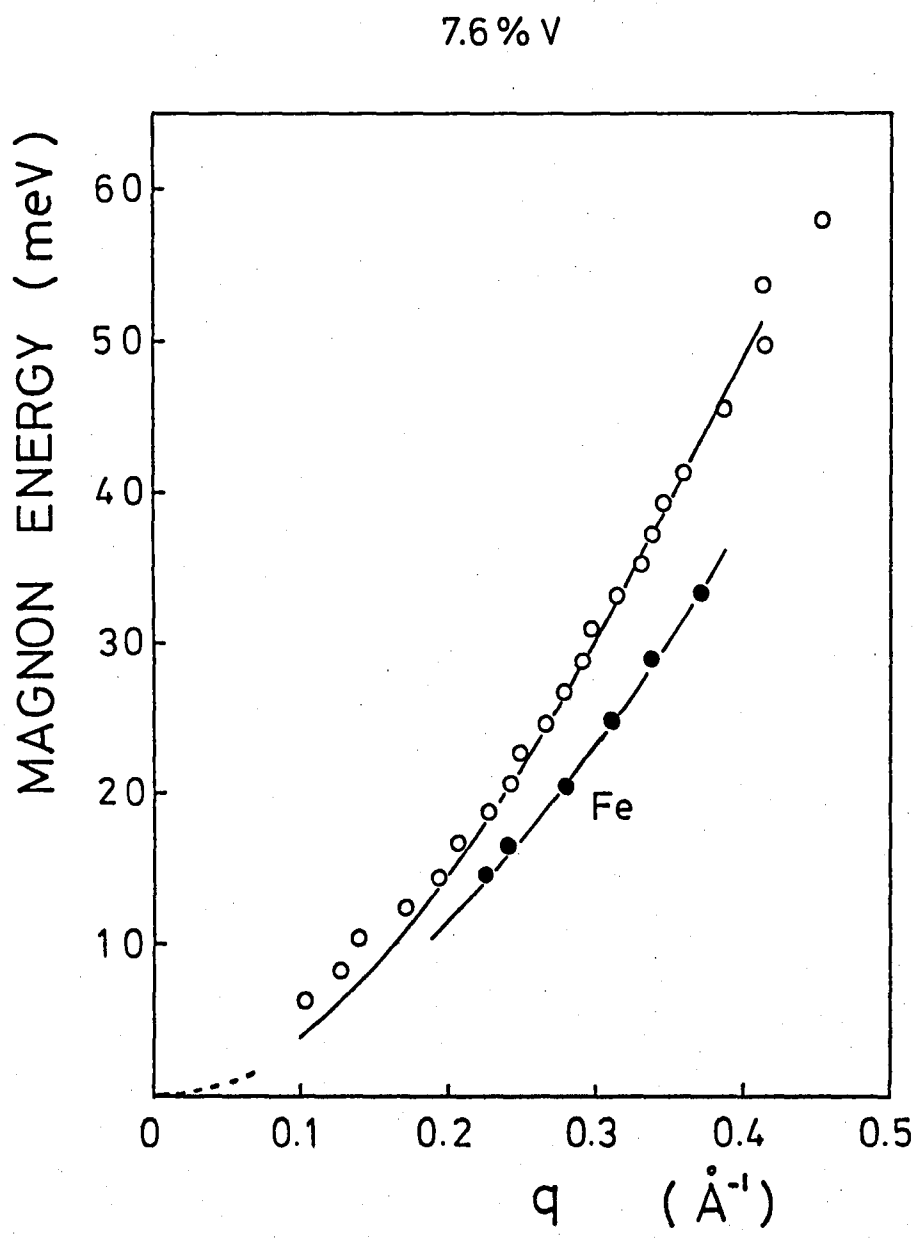

FIGURE 4 (a)

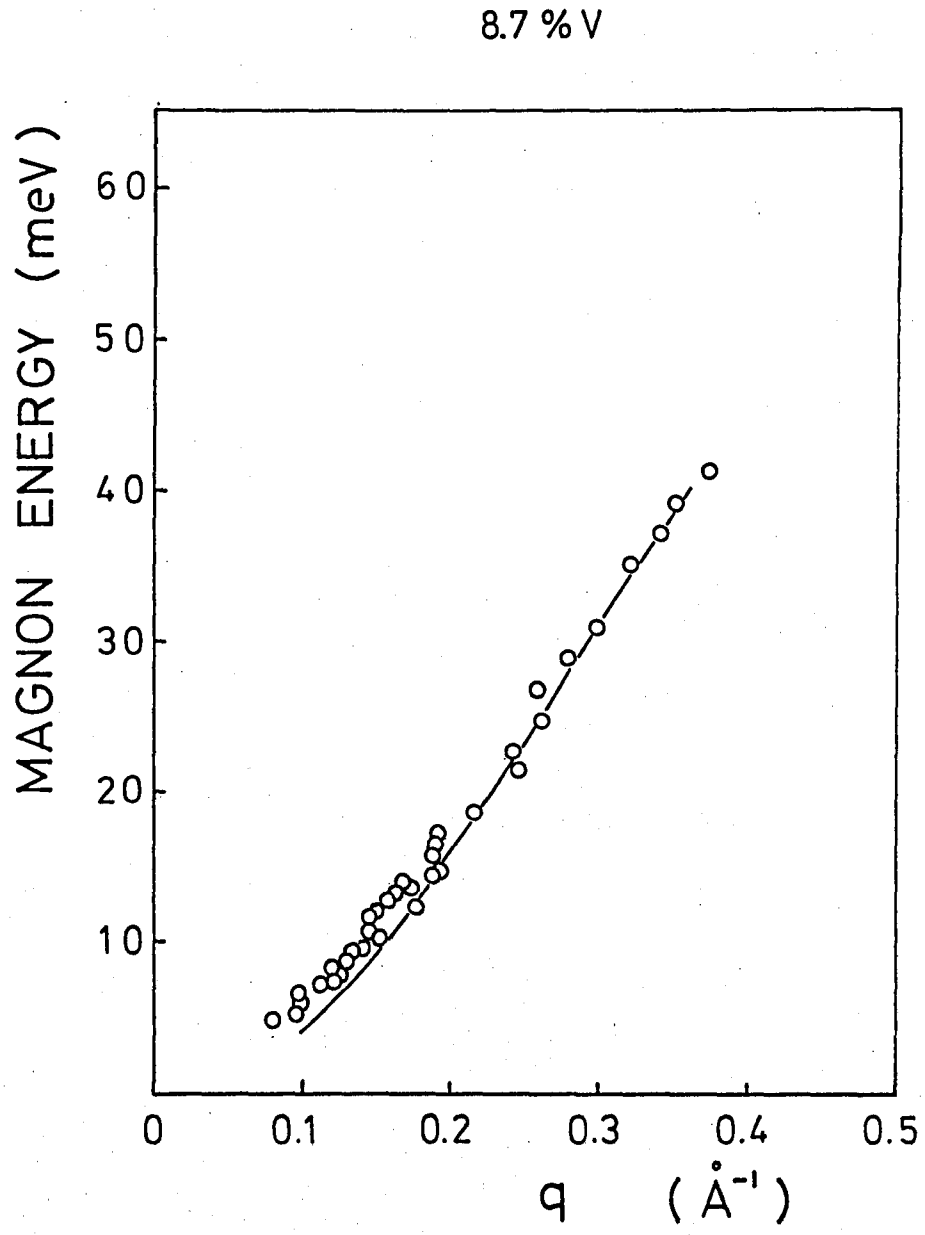

FIGURE 4 (b)

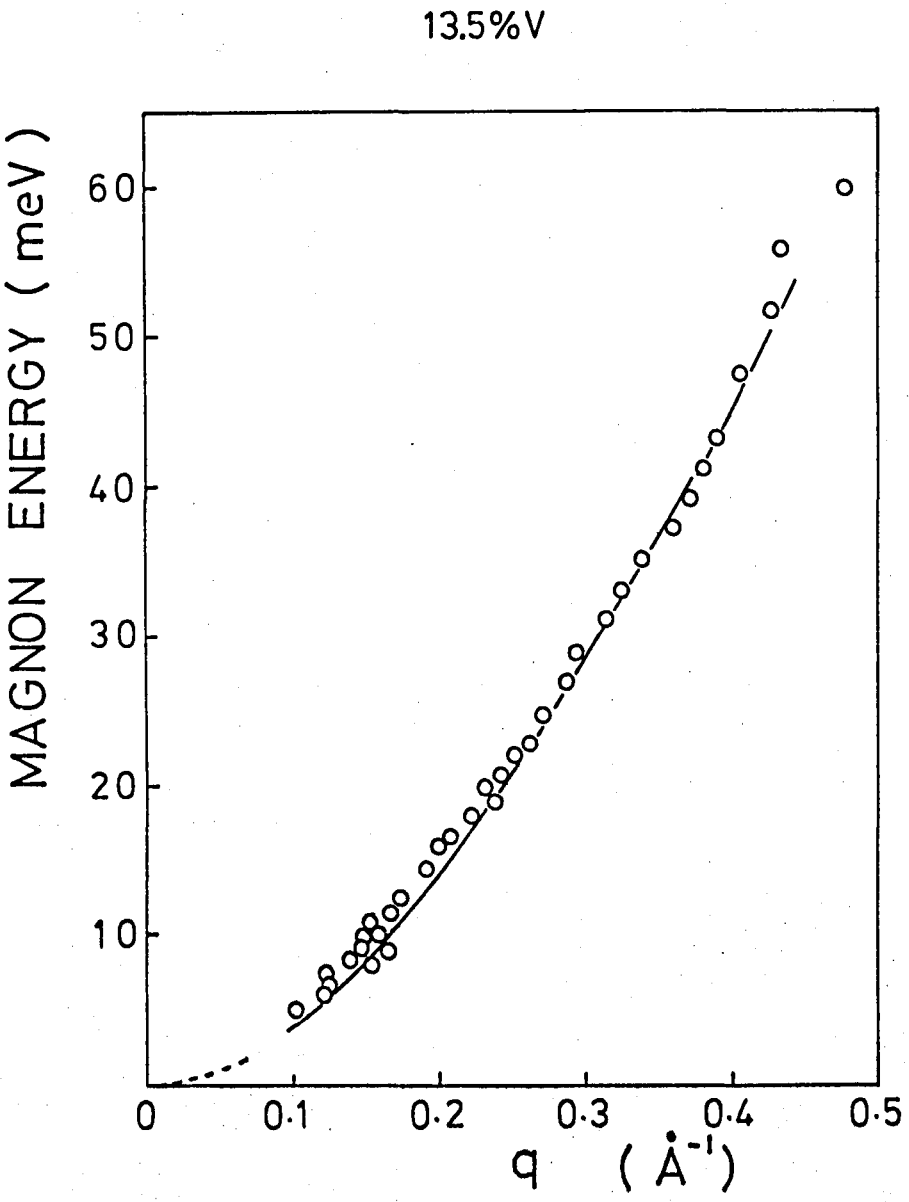

FIGURE 4 (c)

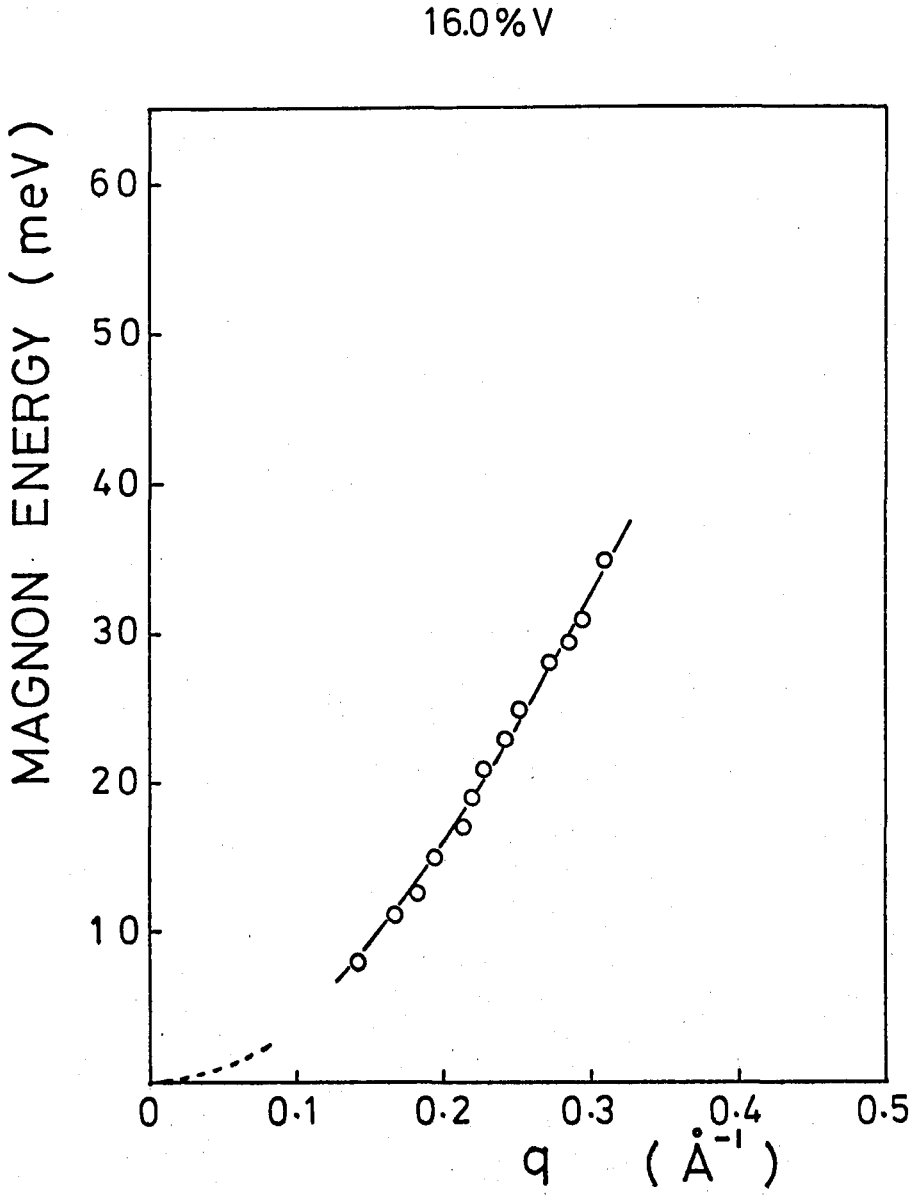

FIGURE 4 (d)

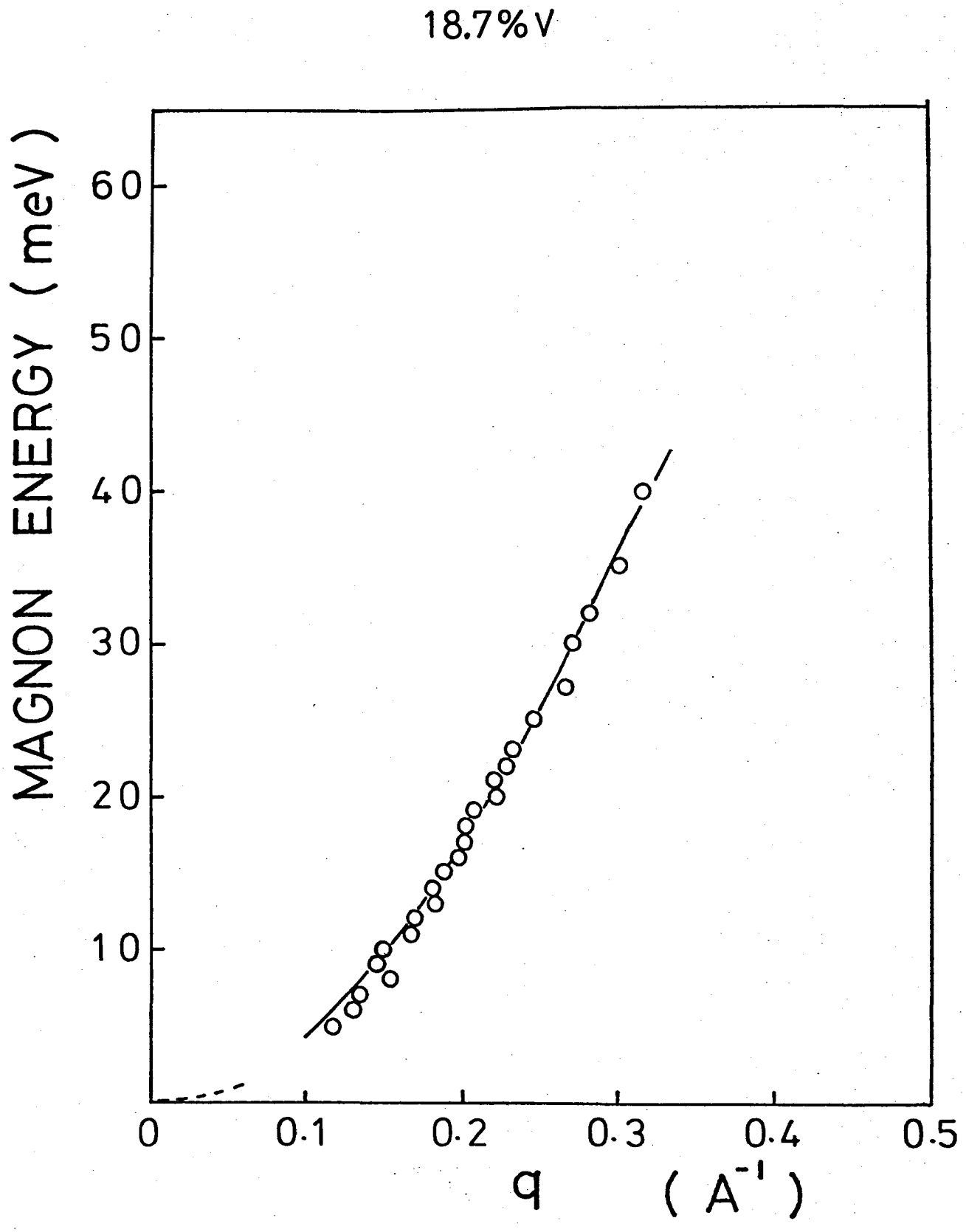

FIGURE 4 (e)

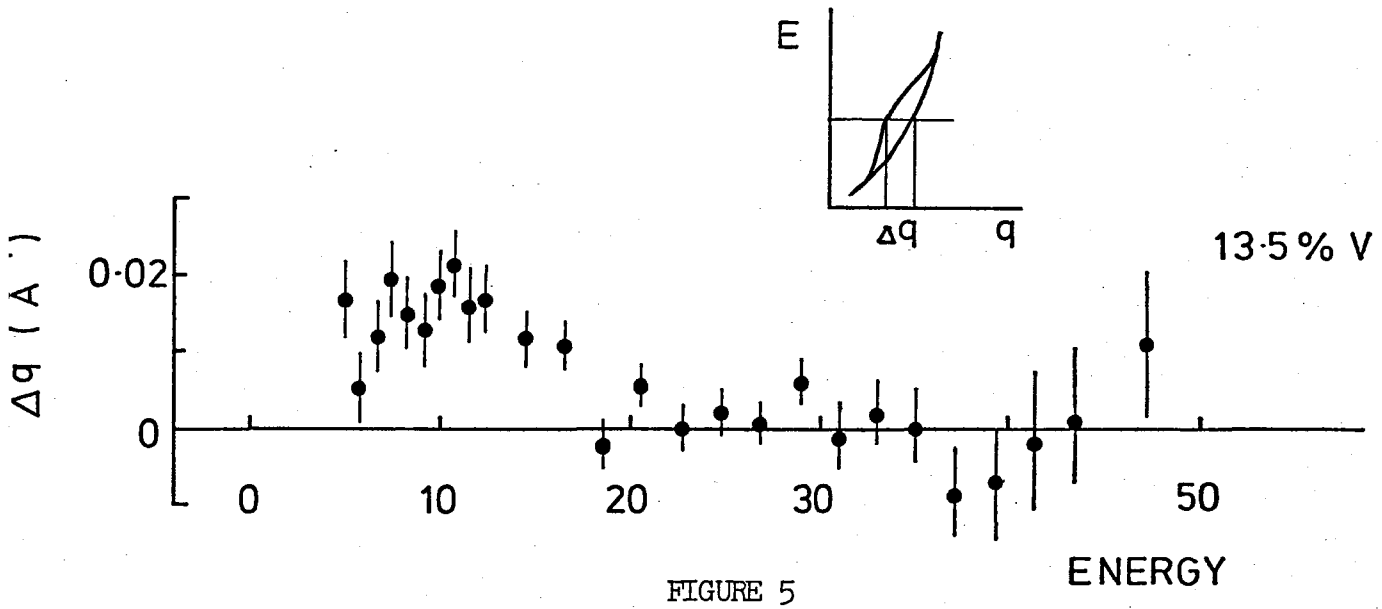

FIGURE 5

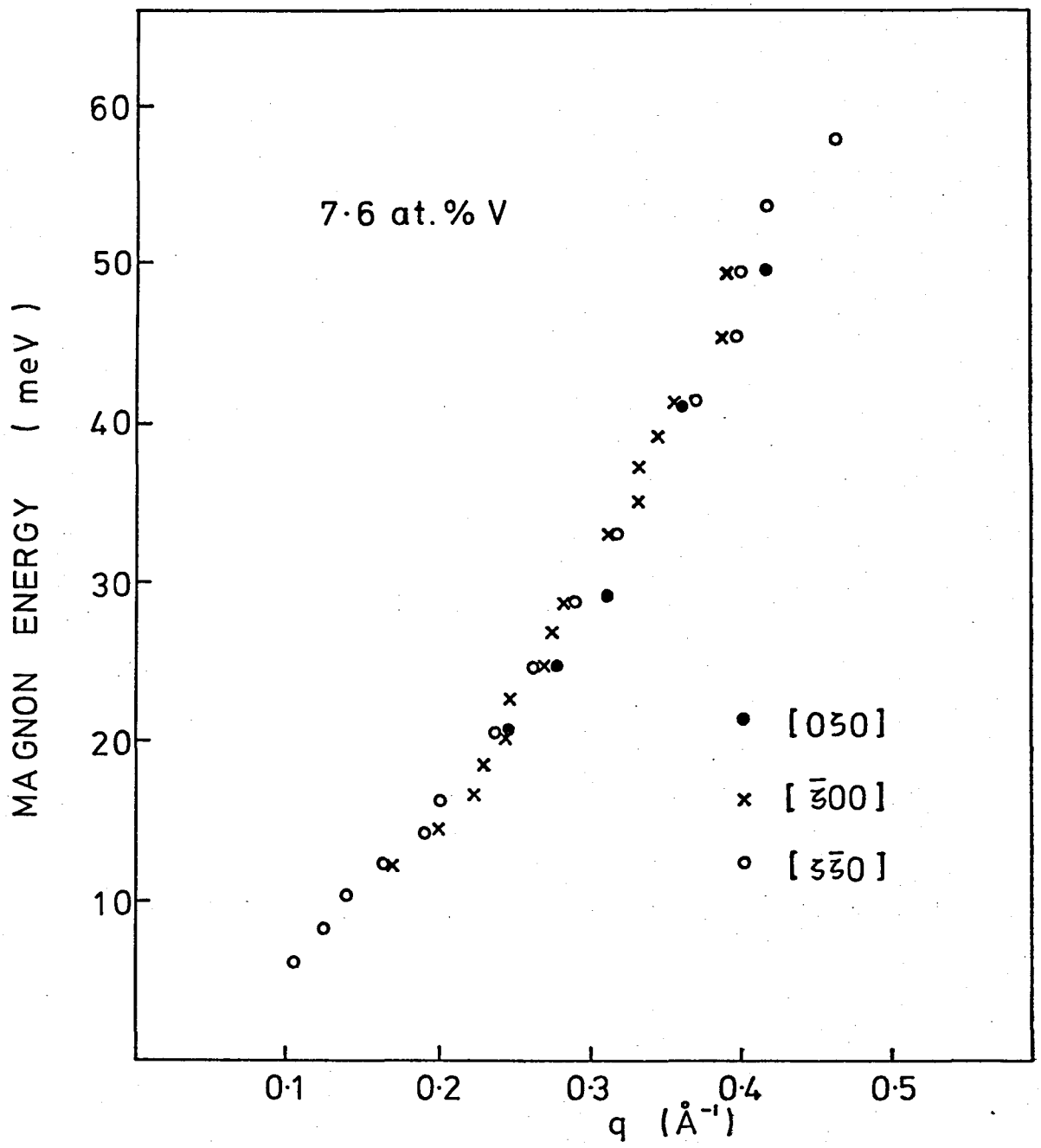

FIGURE 4 (f)

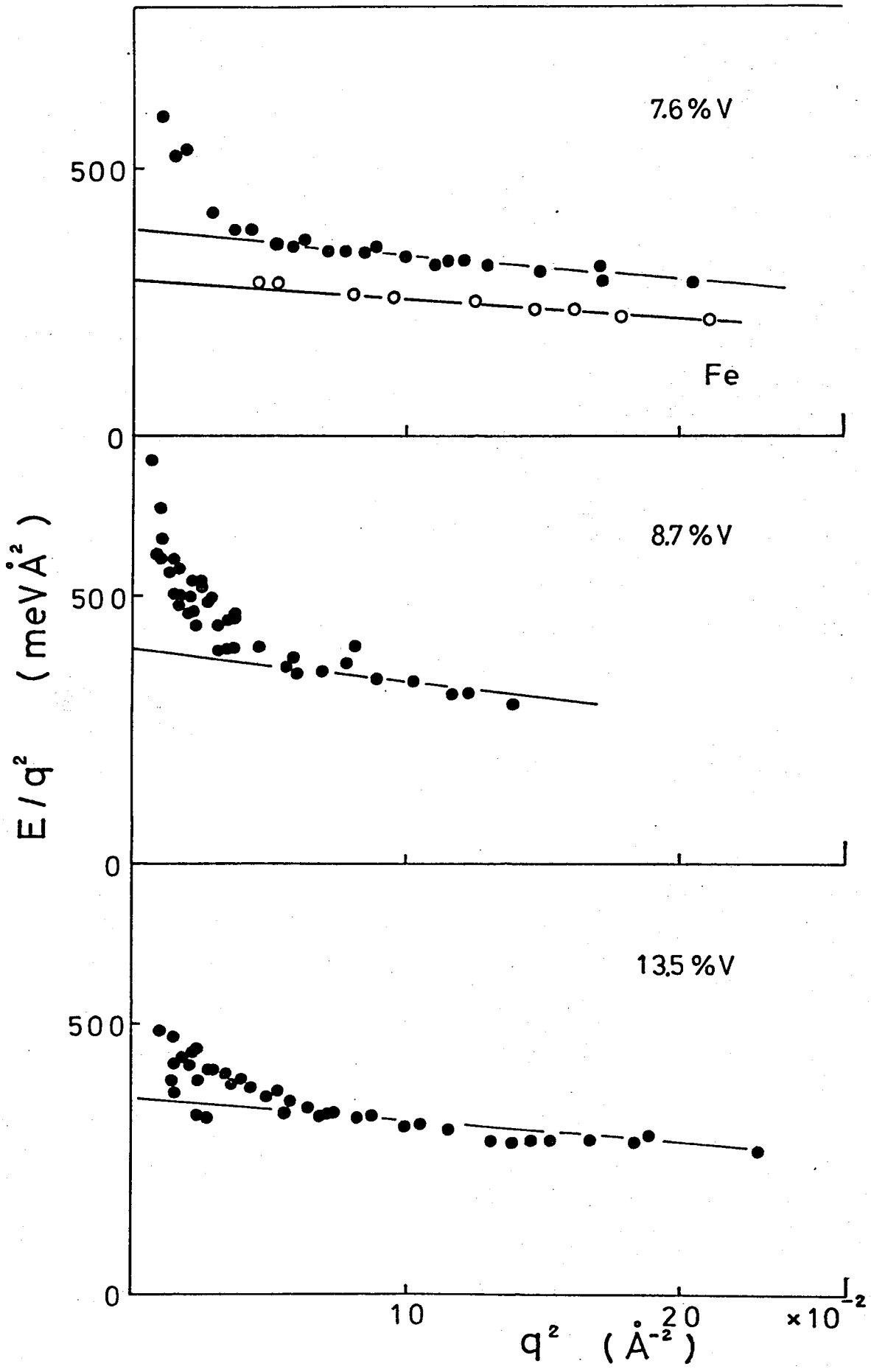

FIGURE 6

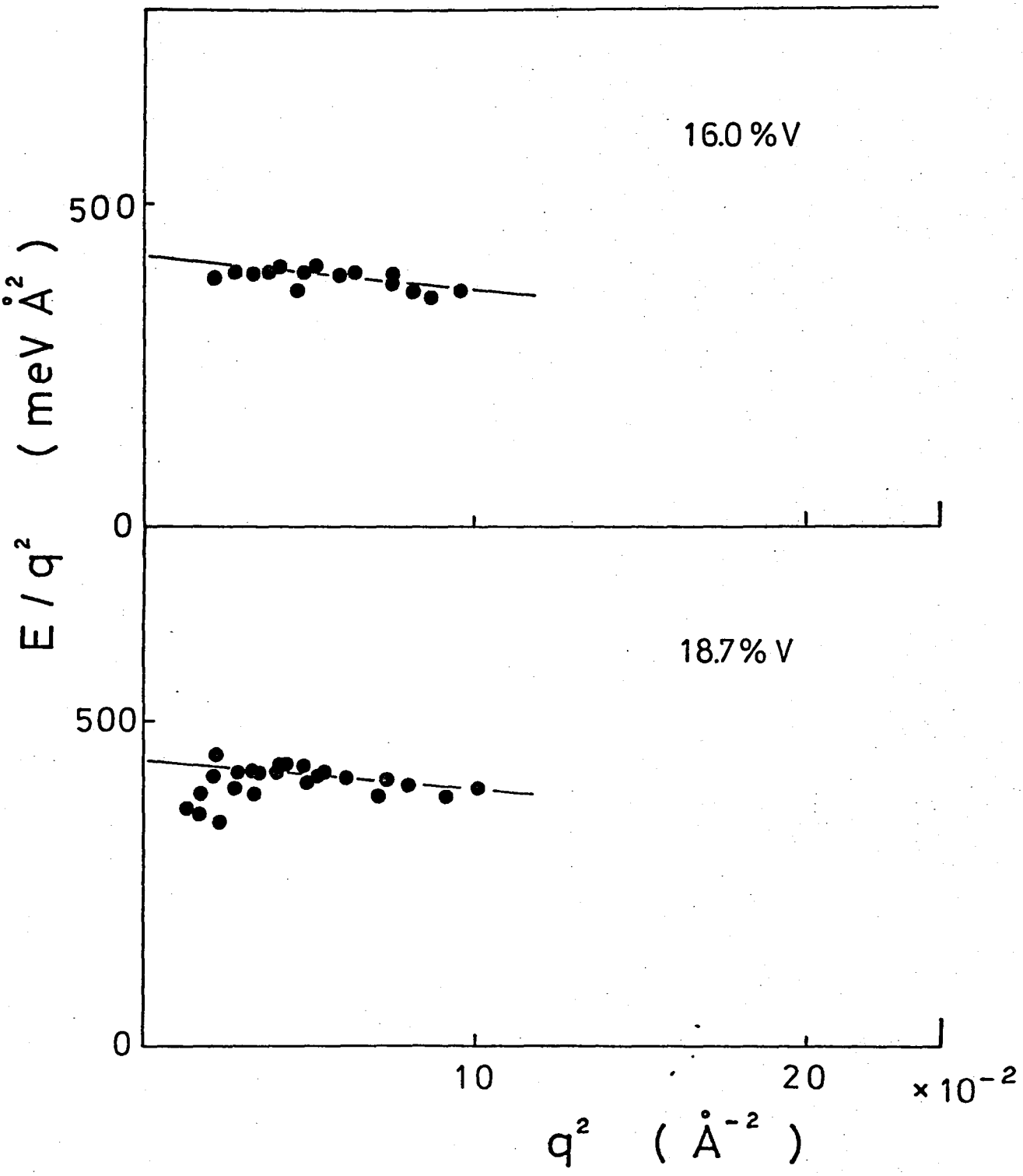

FIGURE 6

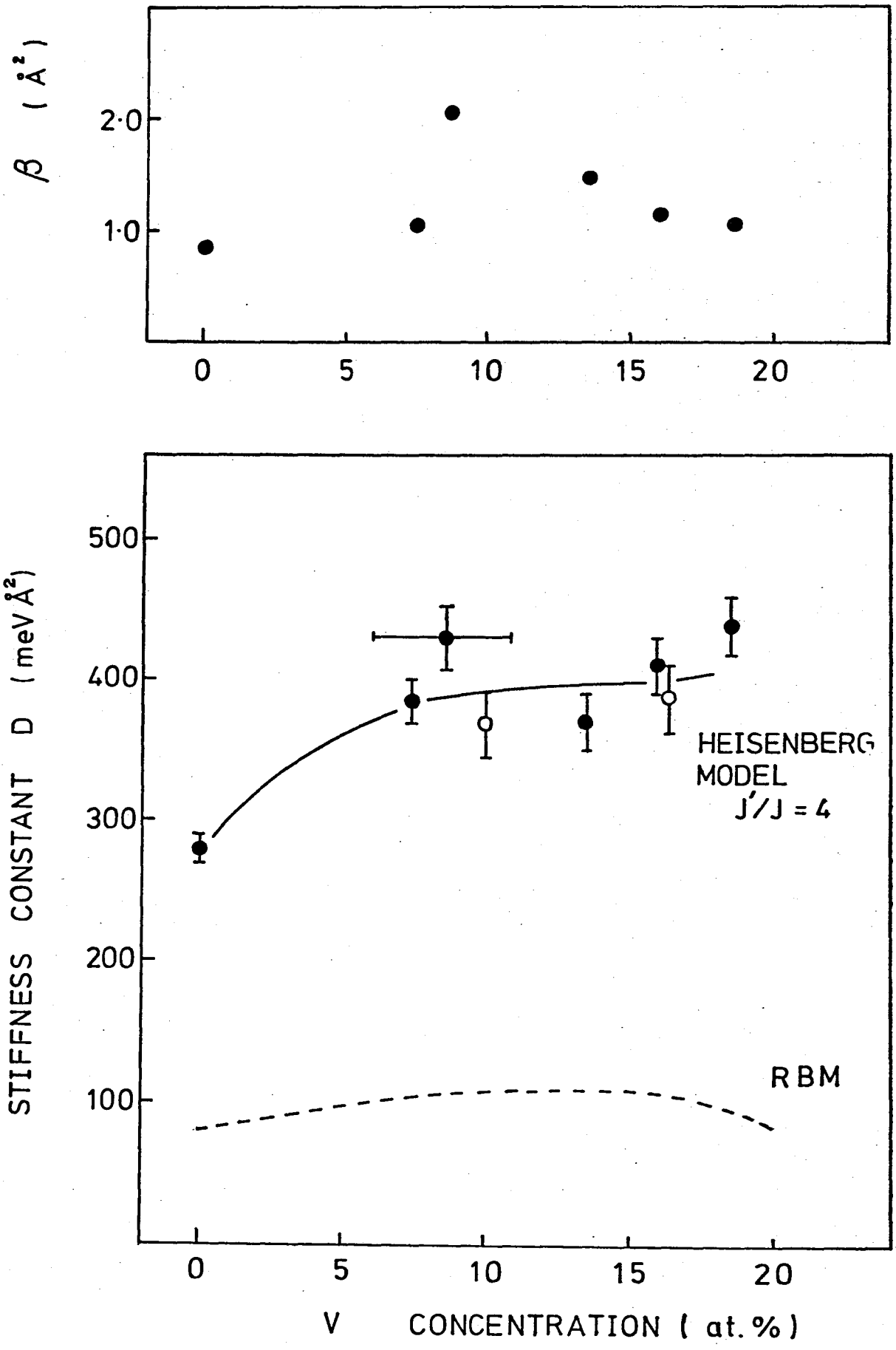
β (Å²)
2·0
1·0
0
5
10
15
20
STIFFNESS CONSTANT D (meV Å²)
500
400
300
200
100
HEISENBERG
MODEL
J'/J = 4
RBM
0
5
10
15
20
V CONCENTRATION (at.%)

FIGURE 7

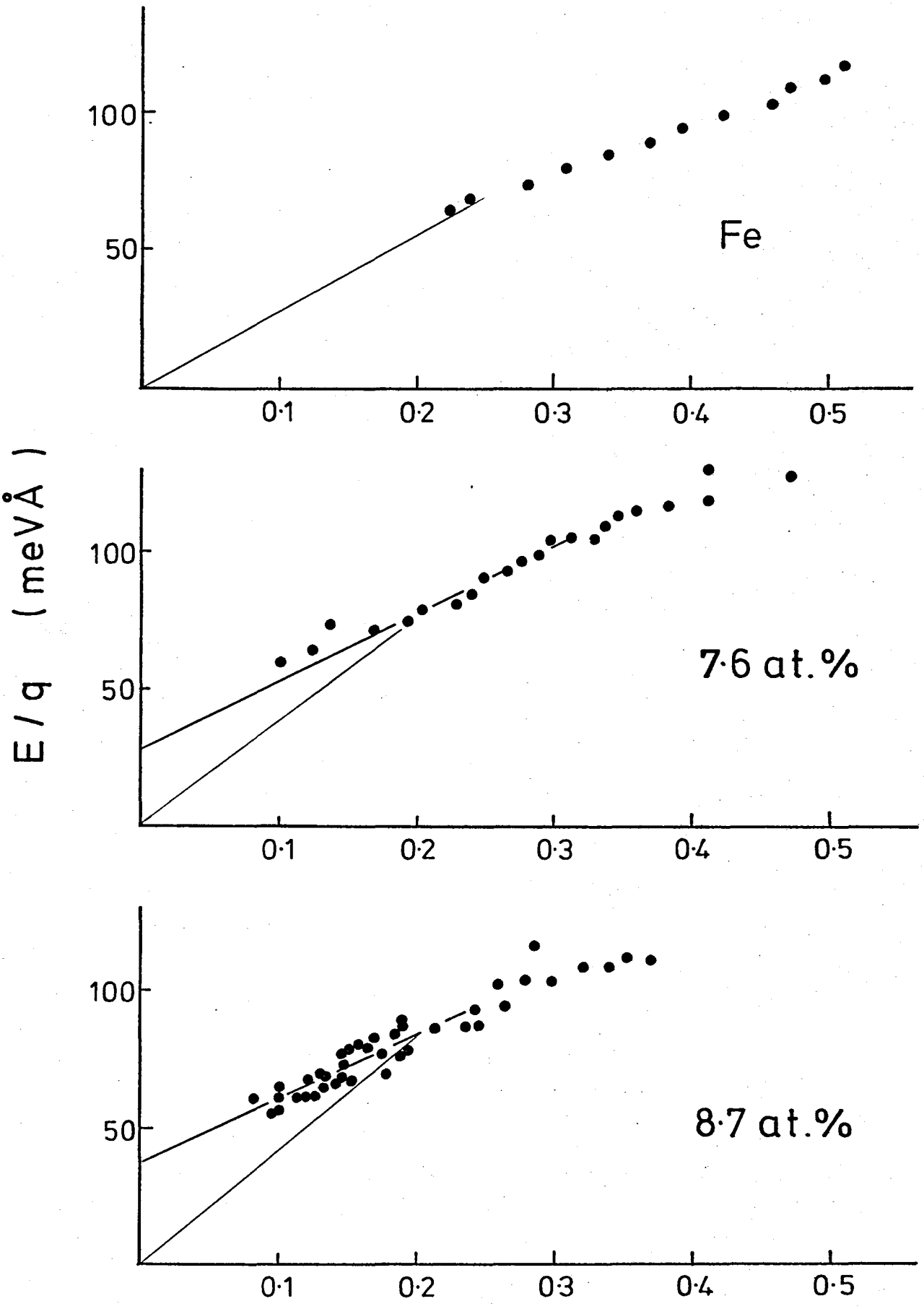

FIGURE 8

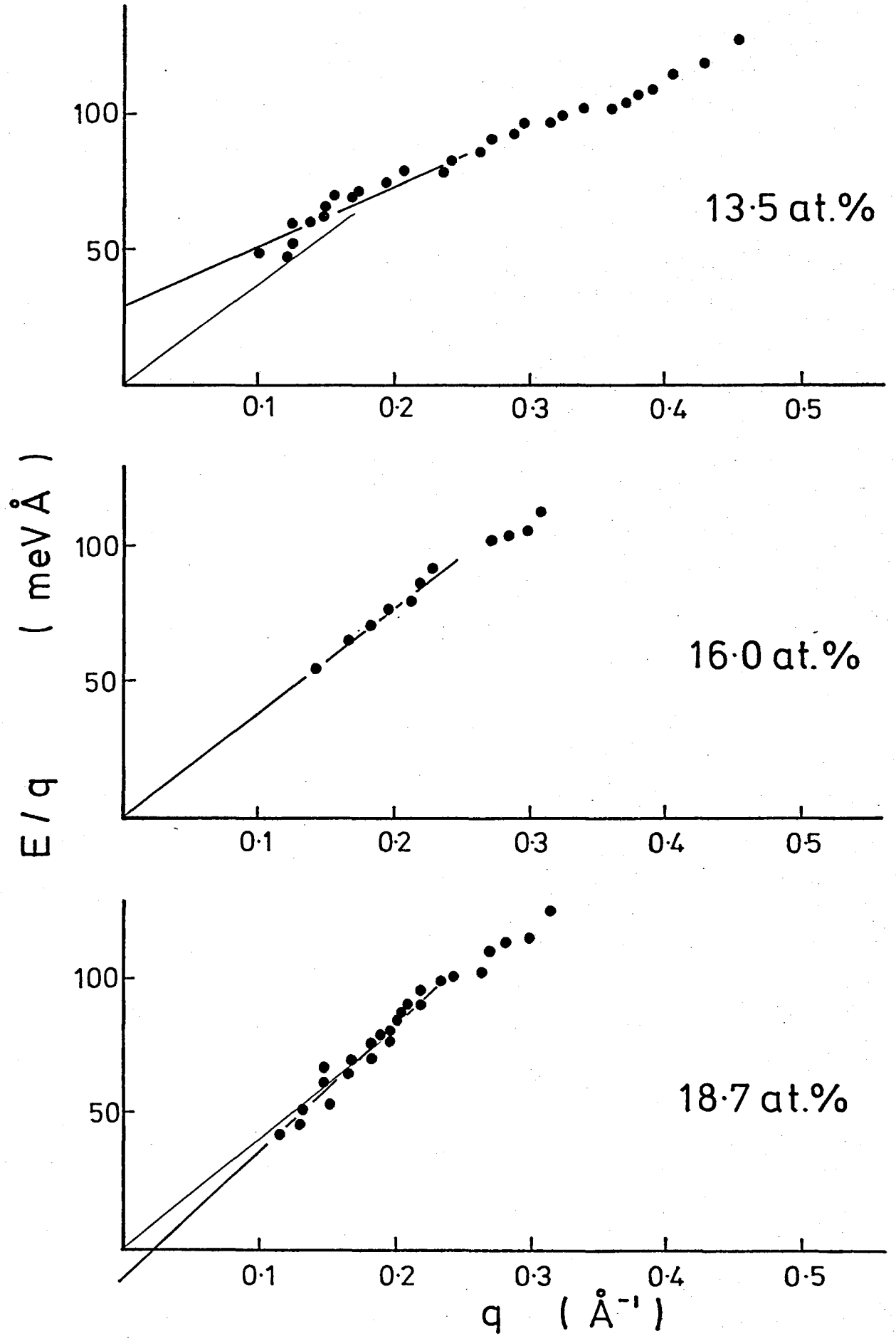
100
50
13·5 at.%
0·1
0·2
0·3
0·4
0·5
E / q (meV Å)
100
50
16·0 at.%
0·1
0·2
0·3
0·4
0·5
100
50
18·7 at.%
0·1
0·2
0·3
0·4
0·5
q (Å⁻¹)

FIGURE 8

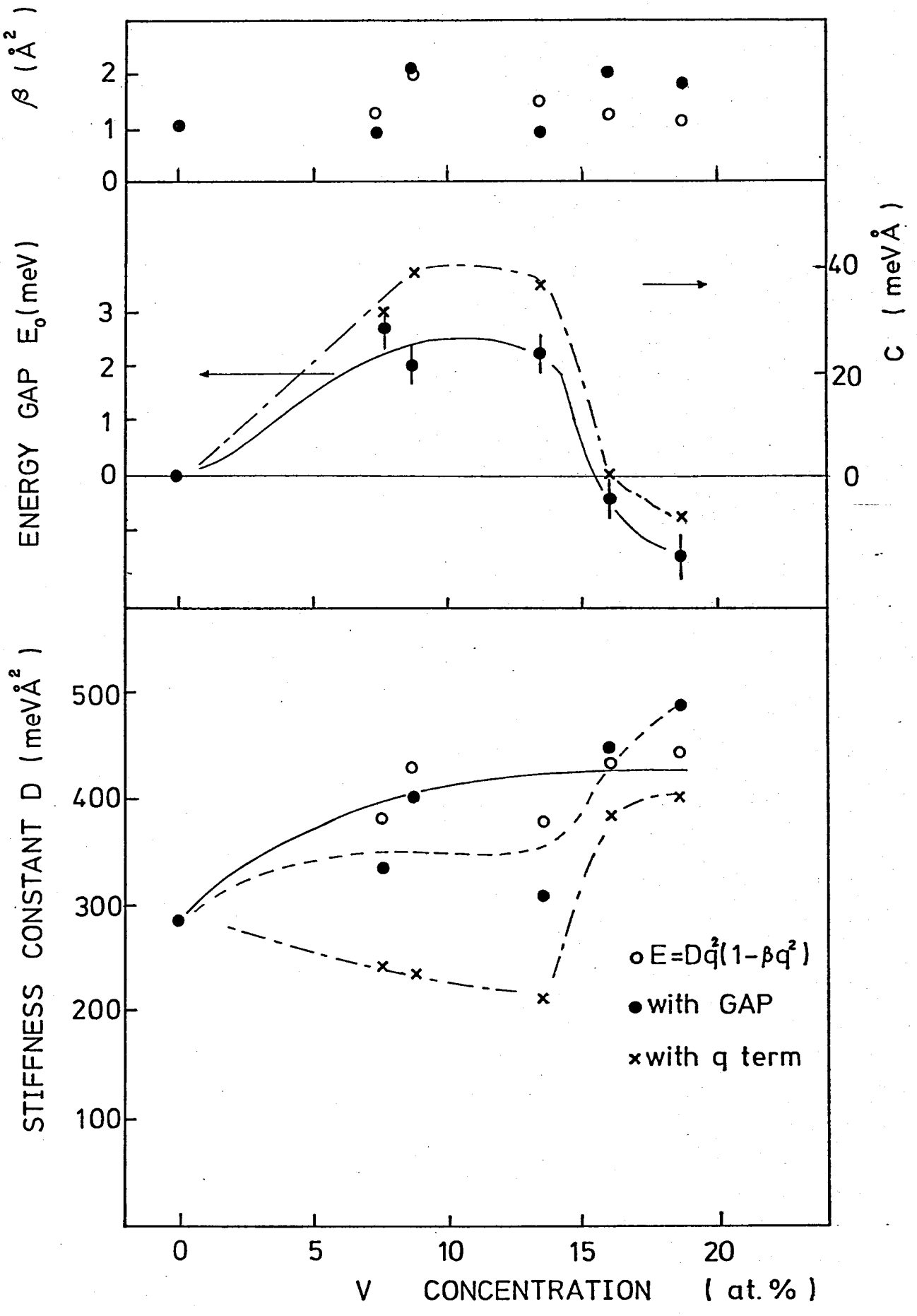
β (Å²)
2
1
0
ENERGY GAP E₀(meV)
3
2
1
0
C (meVÅ)
40
20
0
STIFFNESS CONSTANT D (meVÅ²)
500
400
300
200
100
o E=Dq²(1-βq²)
● with GAP
× with q term
0
5
10
15
20
V CONCENTRATION (at.%)

FIGURE 9

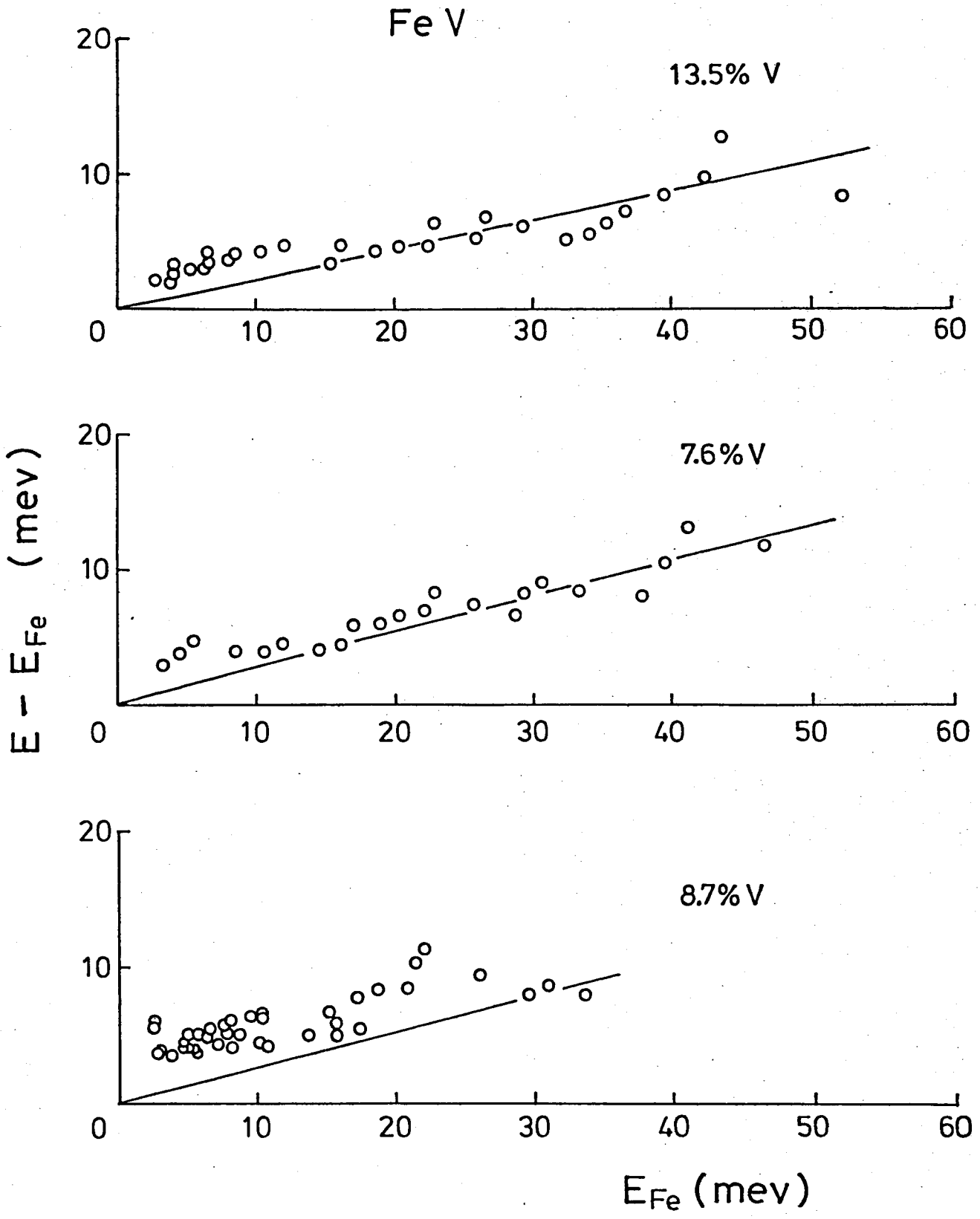

FIGURE 10

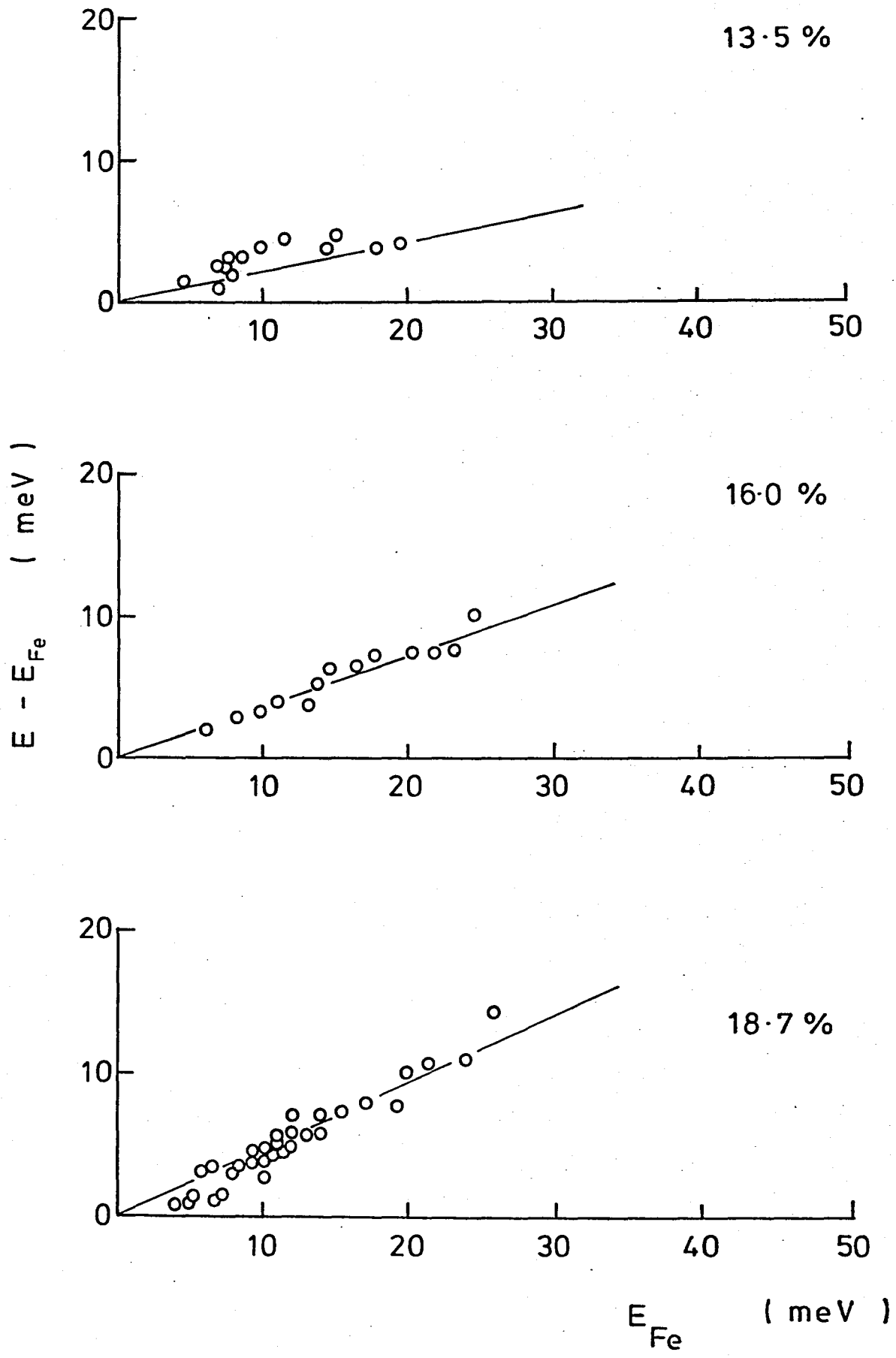

FIGURE 10

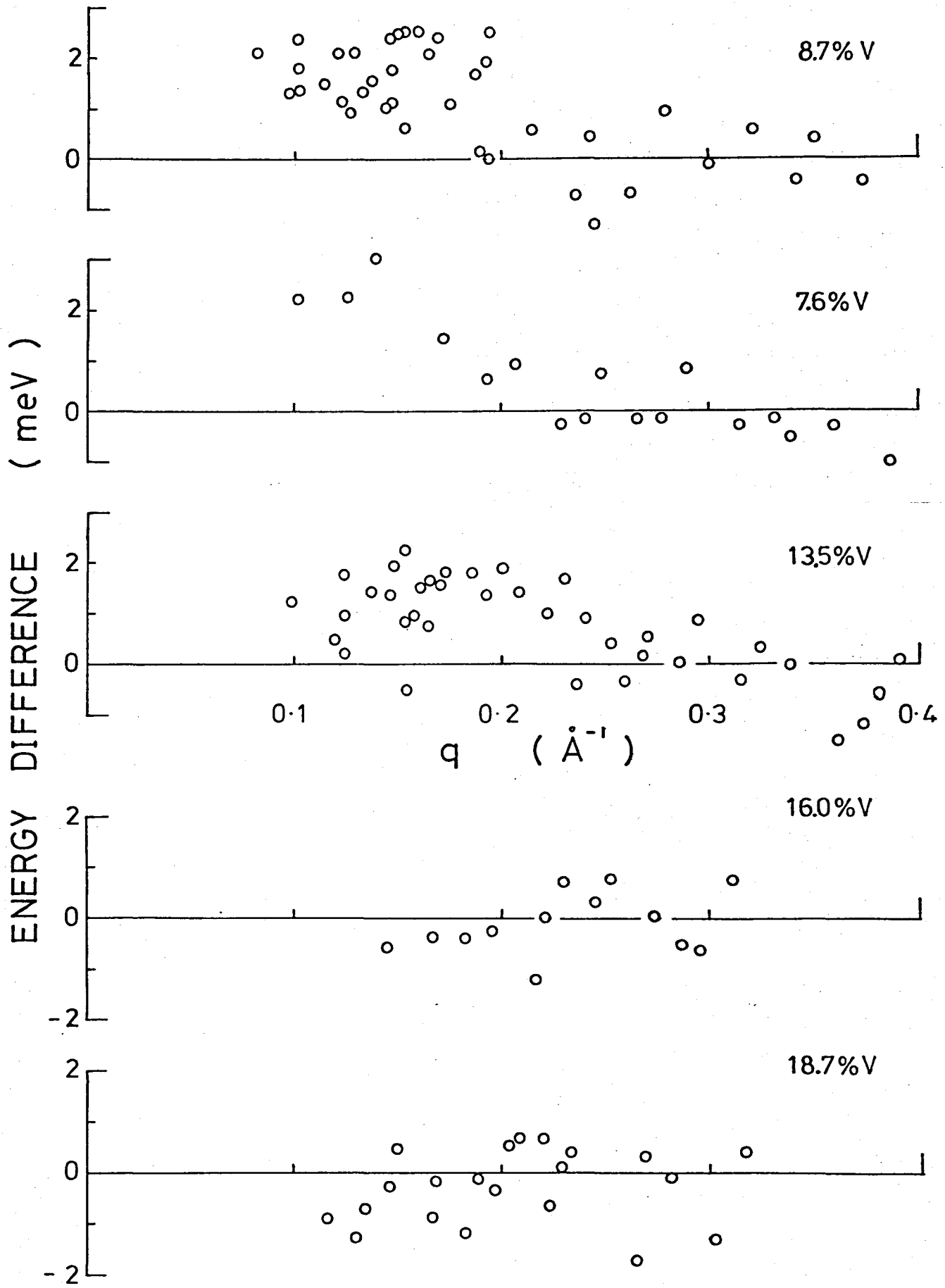
8.7% V
7.6% V
13.5% V
16.0% V
18.7% V
ENERGY DIFFERENCE (meV)
2
0
-2
0·1
0·2
0·3
0·4
q (Å⁻¹)

FIGURE 11

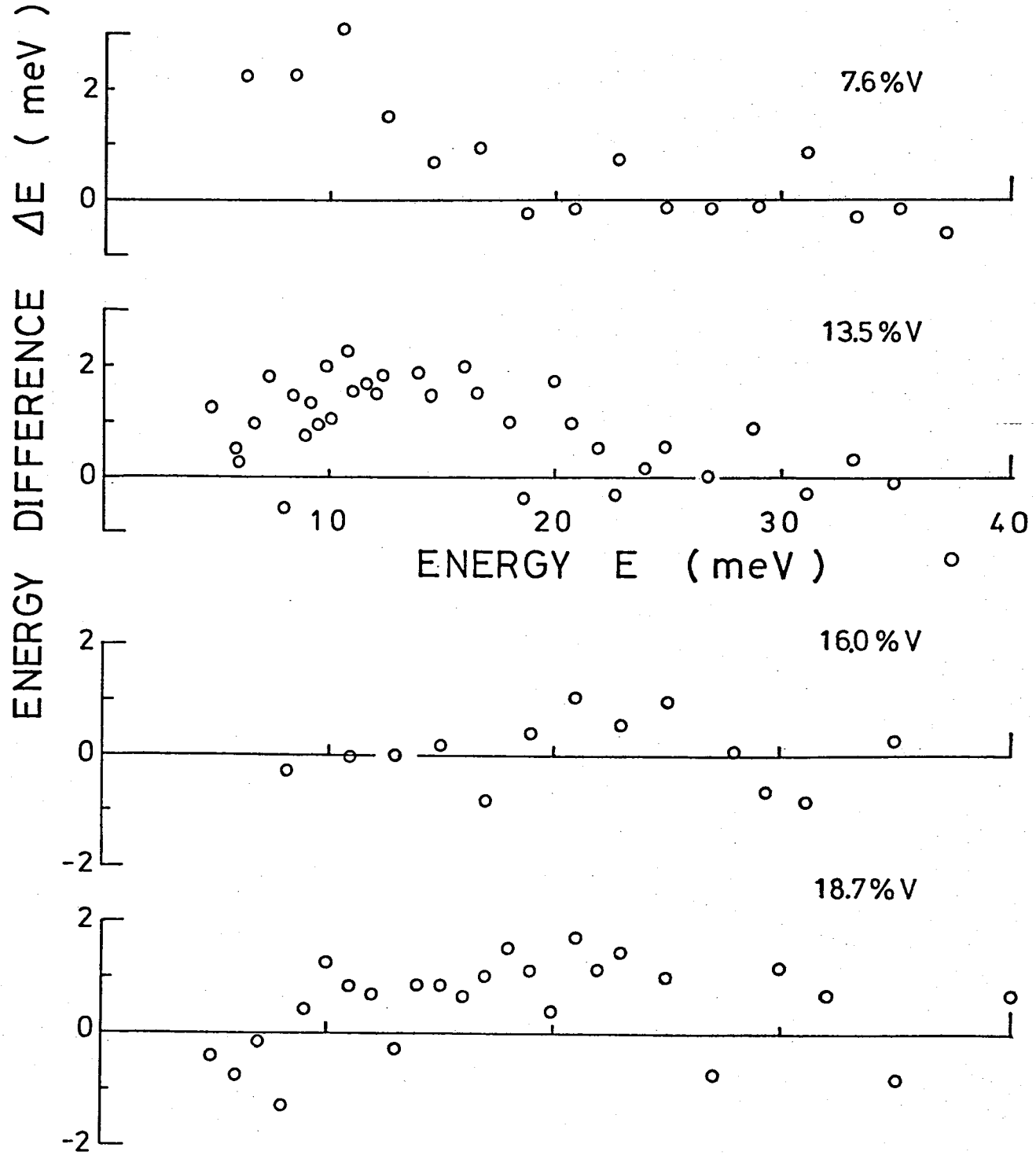
ENERGY DIFFERENCE ΔE (meV)
2
0
7.6%V
13.5%V
10
20
30
40
ENERGY E (meV)
16.0%V
18.7%V
-2

FIGURE 12

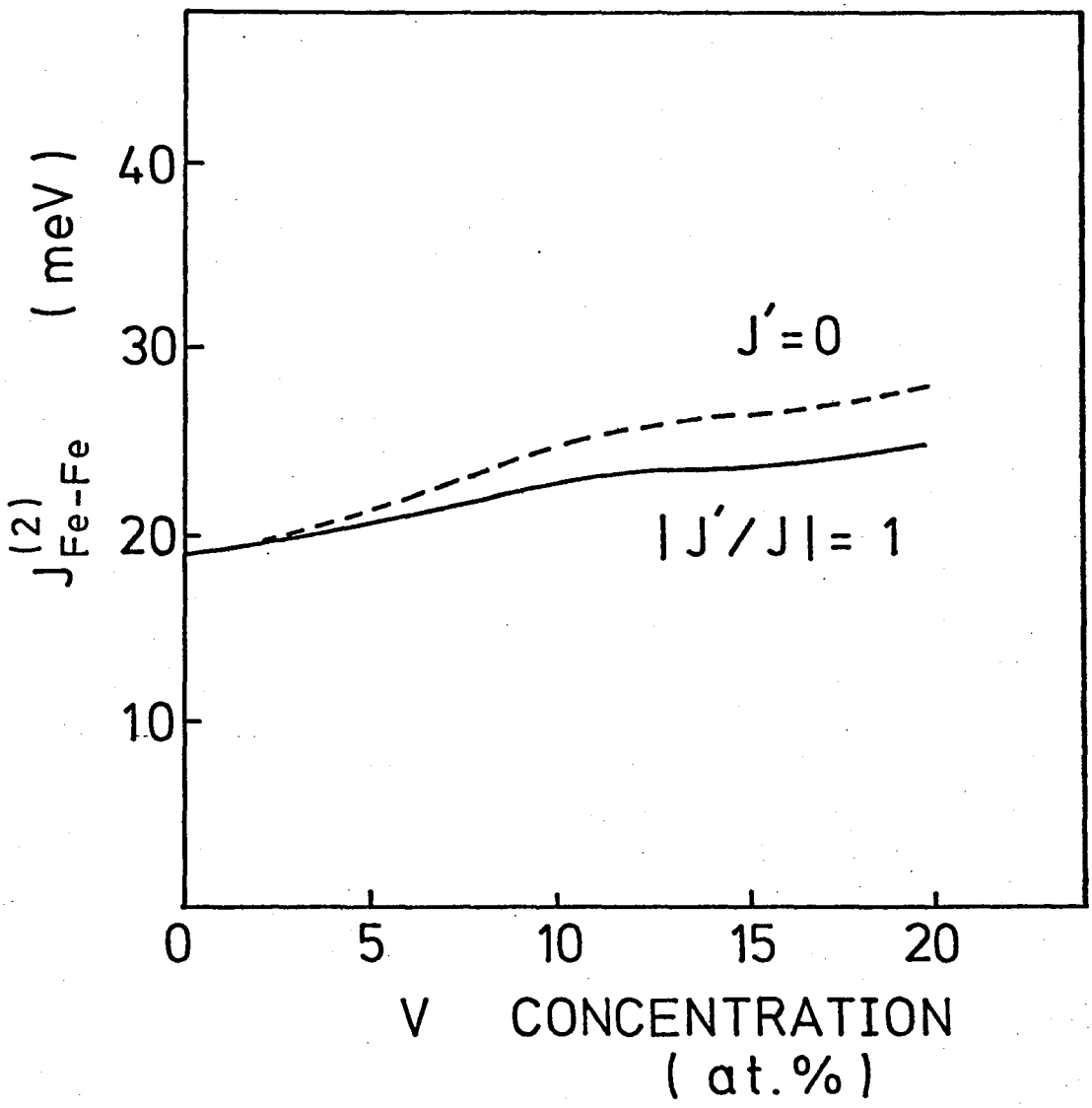

FIGURE 13

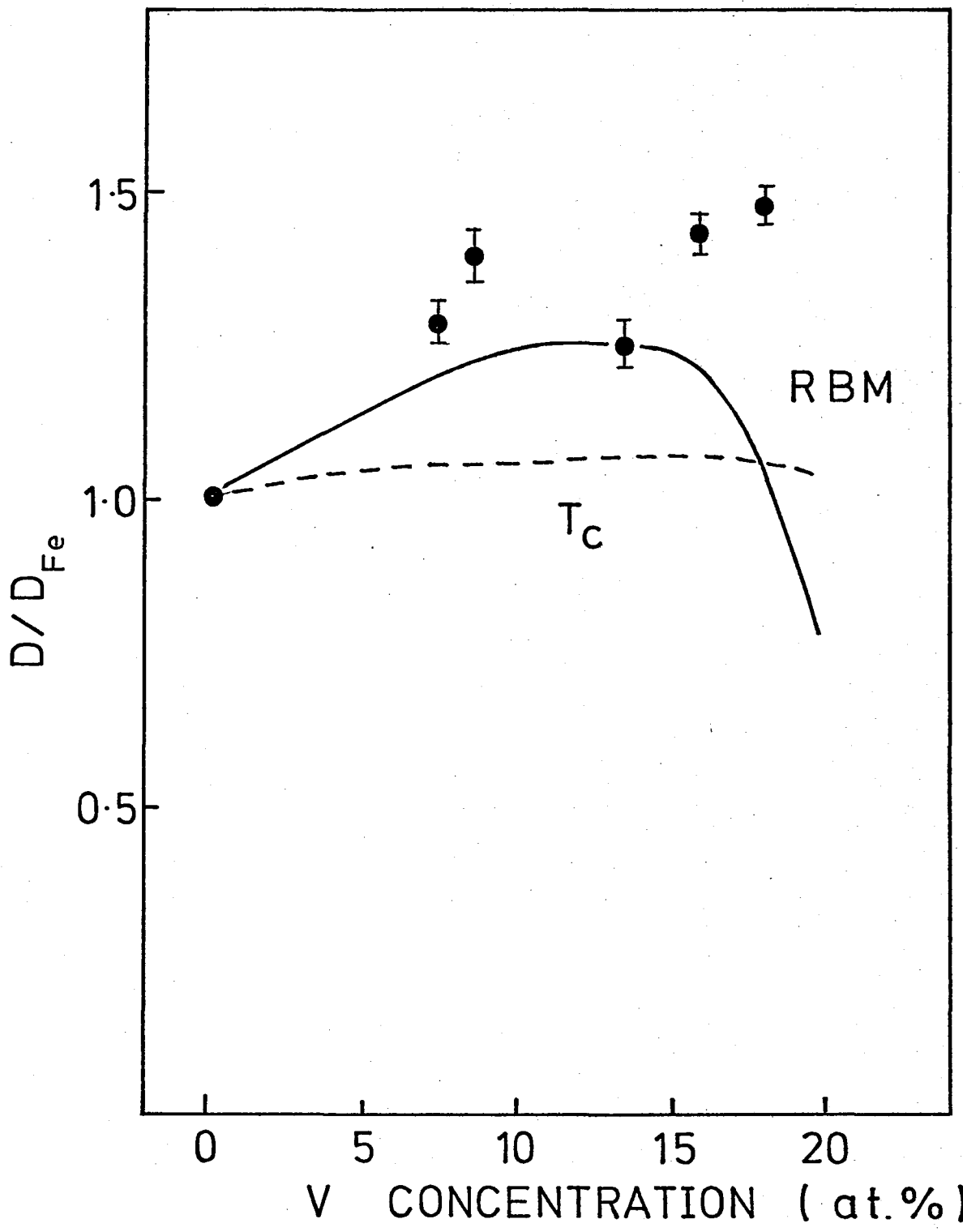

FIGURE 14

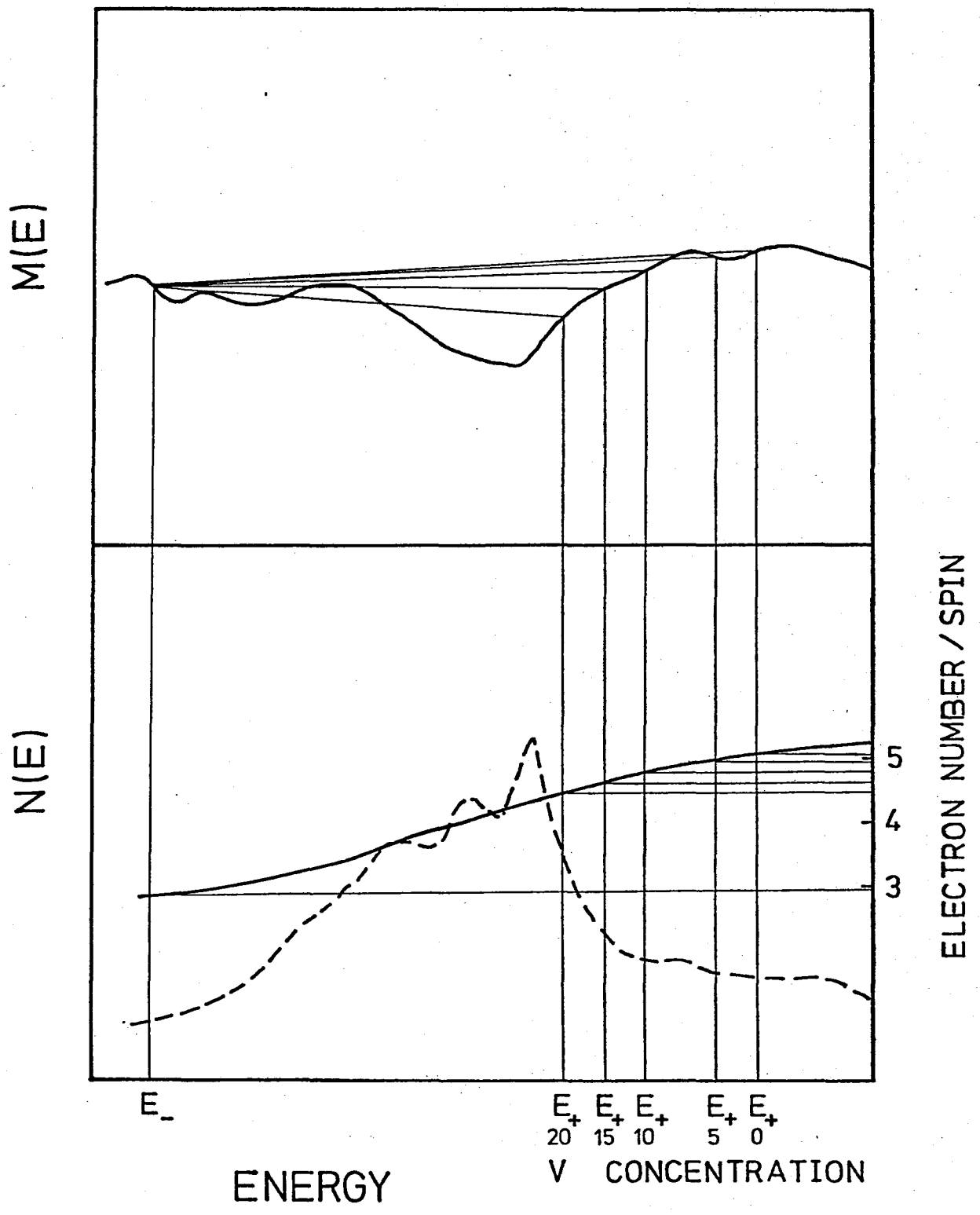
M(E)
N(E)
E_
E+ 20
E+ 15
E+ 10
E+ 5
E+ 0
ENERGY
V CONCENTRATION
5
4
3
ELECTRON NUMBER / SPIN

FIGURE 15

Zusammenfassung

Das Spinswellen Dispersionsverhältnis in den raumzentralen kubischen ungeordneten ferromagnetischen Fe-V Legierungen ist durch die unelastischen Neutronen Streuungen gemessen worden. Die Messungen wurden mit dem drei-achsigen Neutronen Spektrometer an den Proben der 7.6, 8.7, 13.5, 16.0 und 18.7 atomischen Prozent von V in den weiten Bereichen der Anregungsenergie vom 5 bis zum 60 meV an 290 K durchgeführt. Die gemessenen Spinswellen Spektren sind mit der Gleichung $E = D\,q^2(1 - \beta\,q^2)$ auf den relativ größeren Wellenvektorbereichen analisiert. Die Scubmodulkonstante D und β wurden fur die einzelnen Probe bestimmt. Die Größe von D vergrößert sich einst mit der Konzentration von D = 290 meV $\mathring{A}^2$ (von Eisen) , und sättigt sich auf 430 meV $\mathring{A}^2$ an den Probe von 16.0 at.% V. In den niedrigen Energieberich das Dispersionsverhältnis weicht von der oben gegebenen Gleichung ab. Die Abweichung hat die Konzentrationsabhängigkeit. Der Bereich, wo die abweichung der Höchst ist, schiebt sich von der niedrigen zu höheren Energie. Die im Dispersionsverhältnis beobachteten Anomalie mag zu der Effekt der magnetischen Eingesetzte zugeschrieben werden, die der ersten Beispiel beobachtet in den ungeordneten ferromagnetischen Legierungen ist.